Ice-sheet numerical modeling and marine geophysical measurements of glacier-derived sedimentation on the Eurasian Arctic continental margins

Julian A. Dowdeswell* } *Bristol Glaciology Centre, School of Geographical Sciences, University of Bristol,*
Martin J. Siegert } *Bristol BS8 1SS, United Kingdom*

ABSTRACT

Long-range side-scan sonar images of the Barents Sea continental margin have been analyzed in conjunction with results from previous geophysical investigations to determine a qualitative model for sedimentation over the Bear Island and Storfjorden trough mouth fans. These data indicate that gravity-driven debris flows are major processes in the downslope transport of glacial material, delivered to the shelf break when ice sheets advanced across the continental shelf. During late Weichselian time, ~4000 km^3 of sediments were deposited over the Bear Island fan (280 000 km^2) while ~700 km^3 of sediments were deposited over the Storfjorden fan (40 000 km^2). A numerical ice-sheet model, including sediment deformation and transport beneath ice streams, reconstructs the glacial conditions required to transport large volumes of sediment to the late Weichselian Eurasian continental margin. Model results indicate that glaciation of the Eurasian High Arctic occurred after 28 ka, and that ice streams within bathymetric troughs were active by ca. 25 ka. The maximum ice-sheet thickness over the Barents Sea was about 1400 m; there was a secondary dome <1200 m thick over the Kara Sea. Ice extended to the shelf break along the western Barents Sea and Arctic Ocean margins. Ice-sheet decay affected the marine portions of the ice sheet after 15 ka, leaving a northern ice mass between Svalbard and Franz Josef Land that decayed after 13 ka. Ice streams draining ice west and north from the Barents-Kara Sea existed in major bathymetric troughs. Model results predict that ice streams transported sediments to the margin from 27 to 13 ka. Sediment delivery to the margins was generally very high during that time. At 15 ka, the sedimentation rate over the 200-km-wide mouth of the Bear Island trough was ~4 cm yr^{-1} (0.13 cm yr^{-1} averaged over the fan); the rate was 6 cm yr^{-1} (equivalent to 0.6 cm yr^{-1} over the fan) over the Storfjorden trough mouth. The modeled sediment volume at the continental margin of the Bear Island and Storfjorden troughs agrees well with the volumes of late Weichselian sediment inferred from seismic records from these large prograding submarine fans. Sensitivity experiments show that adjustments to model environmental inputs do not significantly affect the results.

INTRODUCTION

During late Cenozoic time on the Norwegian continental margin, major glaciers reaching to sea level first developed about 2.5 Ma, based on the initial occurrence of sand-sized iceberg-rafted debris in marine sediment cores (Jansen and Sjøholm, 1991). Since that time, a series of very large submarine fans has built up along the continental margins of the Norwegian-Greenland Sea (Dowdeswell et al., 1996a; Vorren et al., 1998), separated from one another by areas of much lower sedimentation. Some of these prograding fans have been investigated using seismic and side-scan sonar methods, and their dimensions and architecture have been described and discussed (e.g., Vorren et al., 1989, 1998; Boulton, 1990; Laberg and Vorren, 1996a, 1996b; Hjelstuen et al., 1996; Dowdeswell et al., 1997a). There is also more limited evidence that major fan systems are present on the Arctic Ocean margin of Eurasia, between Svalbard and Severnaya Zemlya (Vågnes, 1996) (Fig. 1).

The major source of sediments to the Eurasian Arctic continental margins over the past 2.5 m.y., and to the fans in particular, is from ice sheets. During a series of glacial-interglacial cycles, ice sheets have built up over the Barents and Kara Seas region, and over Scandinavia (Fig. 1). During full-glacial conditions, these ice sheets reach the continental shelf break, and sediment delivery to the upper continental slope increases rapidly. By contrast, deposition in interglacials, such as Holocene time, comprises only slow hemipelagic sedimentation (e.g., Andersen et al., 1996). The existence of major fans, located at the mouths of prominent cross-shelf troughs, implies that sediment delivery is not uniform along the ice-sheet margin. In modern ice masses, the presence of fast-flowing ice streams between slower moving ridges (e.g., Rose, 1979; Bentley, 1987; Dowdeswell and Collin, 1990) suggests that variations in glacier dynamics are likely to be responsible for regions of enhanced sediment delivery at ice-sheet margins and thus for the development of these major fan systems (Dowdeswell et al., 1996a).

In this paper we combine marine geophysical and geological evidence on the dimensions and rates of build-up of the major submarine fans on the Eurasian Arctic continental margins with numerical modeling of the dynamics of the adjacent ice sheet. The ice-sheet model, in which ice growth and decay are responses to external forcing from climate and sea-level change (e.g., Siegert and Dowdeswell, 1995), provides time-dependent predictions of ice-sheet dimensions and flow rates, together with calculations on the rate of sediment delivery to the continental margin. Using evidence from marine geophysical investigations of the large fans, together with a numerical modeling approach to the prediction of ice-sheet dynamics and sedimentation rates, we test the idea that fan development through time is linked closely to the form and flow of past ice sheets.

*E-mail: j.a.dowdeswell@bristol.ac.uk.

GSA Bulletin; July 1999; v. 111; no. 7; p. 1080–1097; 12 figures; 3 tables.

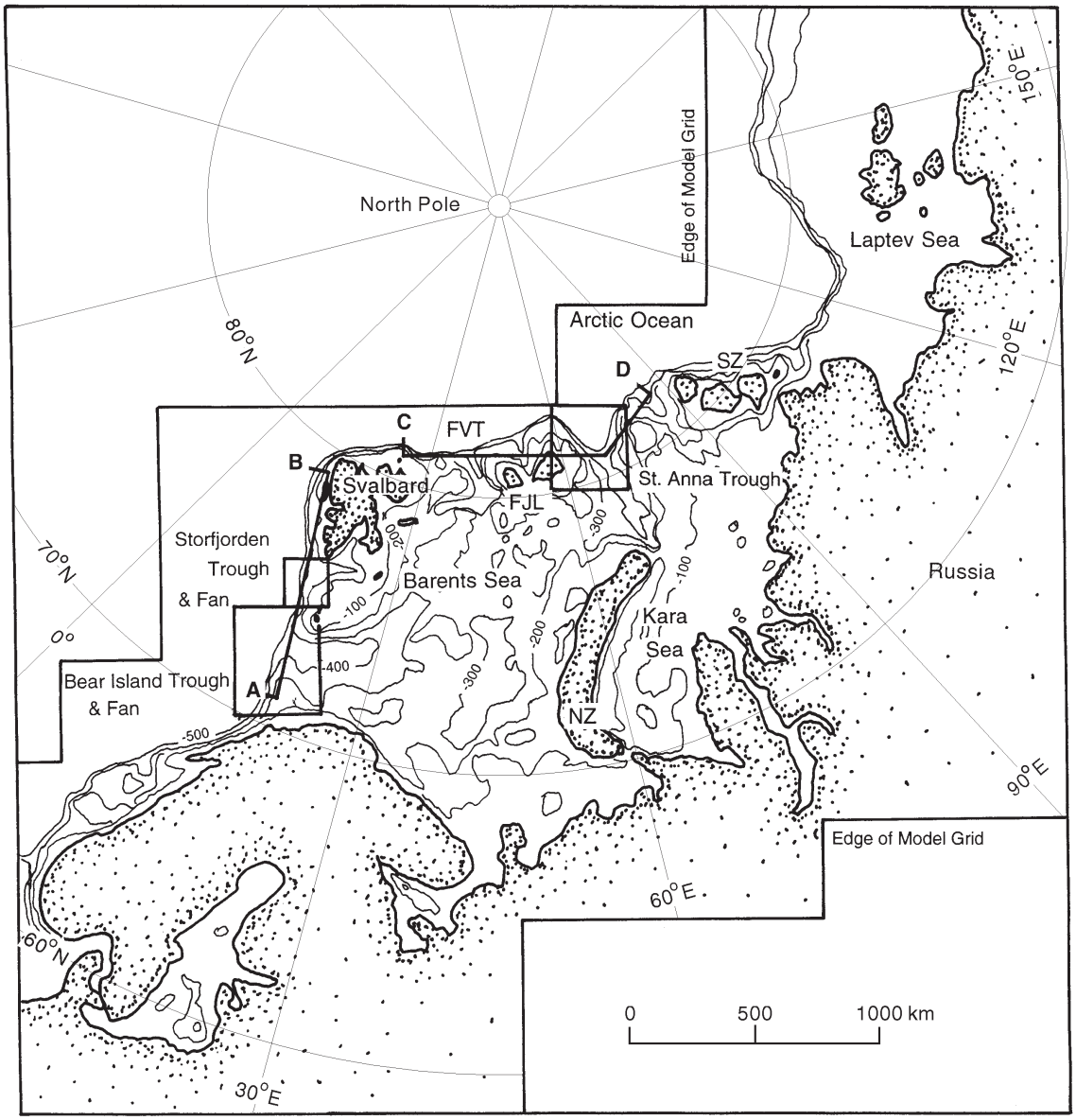

Figure 1. Map of the Eurasian continental margin with bathymetry, area of model grid, and major depocenters of glacier-influenced fans and cross-shelf troughs. The grid consists of 46 200 cells (210 by 220 cells, each 20 km wide). Boxes denote areas over which the sediment volume delivered to the trough mouth fans was determined (see Fig. 10). The areas of the boxes were designed to ensure that all sediment transported to the trough mouth is collected by the model. Note that <90% of the sediment within such boxes is located at the continental margin. Two transects, over which sediment flux at four time slices is calculated (A–B and C–D; see Fig. 11), are also indicated. FJL—Franz Josef Land, SZ—Severnaya–Zemlya, NZ—Novaya Zemlya, FVT—Franz-Victoria trough.

SEDIMENTATION ON THE EURASIAN ARCTIC CONTINENTAL MARGINS

Fan Distribution and Architecture

A series of large, glacier-influenced submarine fans is present on the passive continental margins of the Eurasian Arctic (Fig. 1). The extent and thickness of these fans have been investigated using a combination of geophysical tools, including reflection seismic methods and long-range side-scan sonar systems (Vorren et al., 1998). Each of the fans has formed at the mouth of a cross-shelf trough, some of which are offshore of major fjord systems. The largest is the Bear Island fan, located west of the epicontinental Barents Sea, with an area of ~280 000 km^2 (Fig. 1). A number of other fans are present on the northern Barents and Svalbard margin (Vorren et al., 1998); the Storfjorden fan (40 000 km^2), Bellsund fan (6000 km^2), Isfjorden fan (3700 km^2), and Kongsfjorden fan (2700 km^2). On the East Greenland margin, the Scoresby Sund fan (19 000 km^2) has also been investigated (Dowdeswell et al., 1997a). North of Eurasia, on the Arctic Ocean margin, there is also less detailed evidence of large fans off the Franz-Victoria, St. Anna, and Voronin troughs, between the archipelagos of Svalbard, Franz Josef Land, and Severnaya Zemlya (Vågnes, 1996) (Fig. 1).

These fans appear to have a similar internal architecture, and are made up

of a series of stacked debris flows. The uppermost debris flows are imaged clearly on long-range side-scan sonar records and high-resolution 3.5 kHz profiles (e.g., Vogt et al., 1993; Dowdeswell et al., 1996a). An example of GLORIA 6.5 kHz side-scan sonar imagery and a 3.5 kHz profile from the Bear Island fan illustrate the character of these debris flows in plan and cross section (Fig. 2). The acoustically transparent debris flows range between about 2 and 10 km in width and 10 and 50 m in thickness, and are 30–200 km in length (Dowdeswell et al., 1996a; Elverhøi et al., 1997). In seismic lines over several fans a number of acoustic packages are identified, each made up of a group of stacked debris flows and separated from the underlying packages by a major reflector (e.g., Vorren et al., 1989; Laberg and Vorren, 1995; King et al., 1996). Each acoustic unit is interpreted to represent debris flows from a single glacial-interglacial cycle (Laberg and Vorren, 1995). The debris flows are assumed to be derived from the intermittent failure of clay-rich glacier-derived sediments, deposited on the upper slope during full glacial conditions when the ice-sheet margin was at the shelf break (e.g., Laberg and Vorren, 1995; Dowdeswell et al., 1996a; Elverhøi et al., 1997).

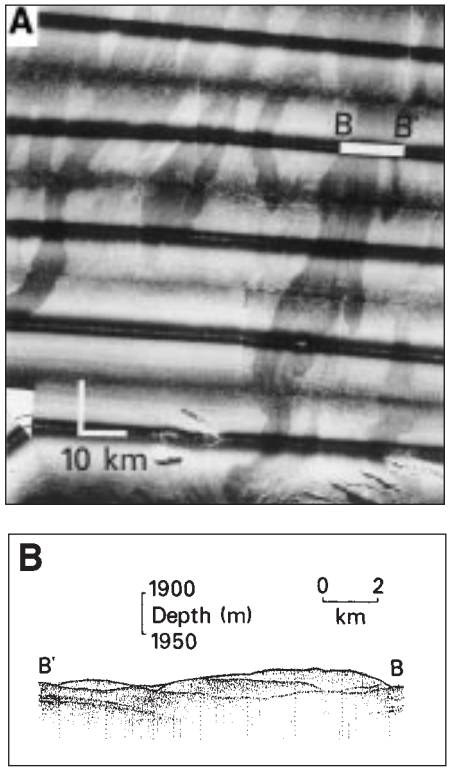

Figure 2. Example of fans and the debris flows that are their building blocks. (A) GLORIA long-range side-scan sonar mosaic of part of the Bear Island fan, showing a series of debris flows on the continental slope with outliers of the mid-Atlantic ridge at the base. (B) 3.5 kHz record showing cross sections of stacked debris flows across the slope of the Bear Island fan.

Volumes and Rates of Fan Deposition

Age-constrained seismic data have been used to construct isopach maps of sediments making up the fans off the Barents Sea continental margin. From these studies, estimates of volume and sedimentation rate for several time intervals have been provided (e.g., Fiedler and Faleide, 1996; Hjelstuen et al., 1996; Laberg and Vorren, 1996a; Solheim et al., 1996). The thickest parts of the glacial sequence, on the Bear Island and Storfjorden fans, are between 3.5 and 4 km, and about 2 km on the Isfjorden fan to the north (Faleide et al., 1996). For the Bear Island fan, Laberg and Vorren (1996a) estimated sedimentation rates of 124 cm/k.y. for the late Weichselian glacial maximum, as compared with only 10–15 cm/k.y. for Holocene time. Over longer periods, Fiedler and Faleide (1996) calculated a total sediment volume of about 340 000 km^3 for the Bear Island fan since about 2.3 Ma, shortly after the onset of Pleistocene glaciation. The average and maximum sedimentation rates over the Bear Island fan, for several time intervals, are given in Table 1 (Fiedler and Faleide, 1996).

Similar seismic stratigraphic studies and isopach mapping on the Storfjorden fan (Fig. 1) have estimated an overall volume of 116 000 km^3 of sediment since 2.3 Ma (Hjelstuen et al., 1996). The average and maximum sedimentation rates over the Storfjorden fan, for several periods, are provided in Table 1 (Hjelstuen et al., 1996). Sedimentation rates on the order of 10–100 cm/k.y. on these two major submarine fan systems contrast with the rate for the earlier Cenozoic, from 55 to 2.3 Ma, when average rates were between about 2.2 and 3.2 cm/k.y. for the Bear Island and Storfjorden margin (Faleide et al., 1996). This difference demonstrates clearly the major role of sediment delivery from ice sheets in the late Cenozoic evolution of the Barents Sea–Svalbard margin.

Geophysical evidence on the long-term rates of glacier-influenced sedimentation on the Bear Island and Storfjorden fans provides valuable data against which to compare the results from our ice-sheet numerical modeling investigations. Sedimentation rates since 440 ka are most relevant to the modeling work, because our ice-sheet model predicts sediment delivery to the continental margin for the late Weichselian period since 30 ka. Even over this interval, a series of accelerator mass spectrometry (AMS) radiocarbon-dated cores from the Svalbard margin shows that ice extended onto the continental shelf for about 10 k.y. and was at the shelf edge for only about 3–4 k.y. (Elverhøi et al., 1995; Andersen et al., 1996). We make two assumptions: (1) ice was at the shelf break for about 10% of each glacial cycle of about 100 k.y. in length, remembering that there may have been more than one advance in each cycle (Mangerud and Svendsen, 1992); and (2) the vast bulk of sediment is delivered to the margin under such full-glacial conditions. The latter statement is supported by both the low observed rates of Holocene sedimentation and the seismic architecture of the fans, where the majority of sediments are from debris flows (e.g., Andersen et al., 1996; Laberg and Vorren, 1996a). A core penetrating the flanks of lens-shaped debris flows on the Isfjorden fan, composed of homogeneous diamicton, yielded AMS reservoir corrected dates of 19 205 ± 210 and 19 195 ± 225 yr B.P. for the base of the debris flows (Andersen et al., 1996). A date of 17 460 ± 145 yr B.P. was also obtained from a debris flow on the Bear Island fan, and is interpreted to represent a maximum age for this flow (Laberg and Vorren, 1995). The dates on both debris flows support the suggestion that they are associated with full-glacial conditions.

The long-term sedimentation rates for the Bear Island and Storfjorden fans can be regarded as measures of full-glacial sediment delivery, which operated over ~10% of the 440 k.y. time interval. This increases the mean and maximum sedimentation rates on each of the fans during full glacials to the following values: a mean of 13 cm /k.y. and maximum of 124 cm /k.y. for the Bear Island fan (Laberg and Vorren, 1996a); and a mean of 29 cm/k.y. and a maximum of 172 cm/k.y. for the Storfjorden fan (Laberg and Vorren, 1996b). Thus, for the late Weichselian glaciation, 4200 km^3 of sediments were deposited in 12 k.y. over the 280 000 km^2 area of the Bear Island trough mouth fan (Laberg and Vorren, 1996a), and 700 km^3 was deposited in 10 k.y. over the 40 000 km^2 Storfjorden trough mouth fan (Laberg and Vorren, 1996b). These volumes and sedimentation rates are used in subsequent comparison with numerical model predictions.

TABLE 1. MEAN AND MAXIMUM SEDIMENTATION RATES OVER THE BEAR ISLAND TROUGH MOUTH FAN (280 000 km^2) AND THE STORFJORDEN TROUGH MOUTH FAN (40 000 km^2)

Time period	Bear Island TMF		Storfjorden TMF	
	mean	max	mean	max
	cm kyr^{-1}		cm kyr^{-1}	
10–20 ka			172	n/a
12–24 ka	124	n/a		
0–440 ka	45	250	25	91
44 ka–1 Ma	172	339	126	337
1 Ma–2.3 Ma	37	93	63	177

Notes: TMF—Trough Mouth Fan. Maximum rates represent the maximum thickness in the depocenter of each seismic unit after Fiedler and Faleide (1996); Hjelstuen et al. (1996); Laberg and Vorren (1996a, 1996b); Vorren et al. (1998).

Qualitative Model for Sedimentation on Glacier-Influenced Margins

A conceptual model for glacier-influenced sedimentation on high-latitude continental margins (Fig. 3) summarizes the role of ice-sheet extent and dynamics on the geographic location and rate of sediment build-up (Dowdeswell et al., 1996a). The model is based on a large volume of long-range side-scan sonar and seismic data from the Polar North Atlantic. During interglacial and interstadial periods, ice is far from the continental shelf edge, and sedimentation on the outer shelf and slope is low and hemipelagic in character. However, in full glacial and some stadial periods, ice advances onto the shelf and across it to the shelf break (Fig. 3, A and B). Ice-stream activity is most likely within bathymetric troughs, because basal temperatures are more likely to reach the melting point in these regions of relatively thick ice, and a reduction in basal drag may occur as a result of low buoyancy-induced effective basal pressures in such areas (Bentley, 1987). Thus, the largest ice sheet was characterized by a series of ice streams situated within troughs that fed ice to the shelf break (Fig. 3A). Most modern Arctic ice streams are located in subglacial troughs (e.g., Dowdeswell and Collin, 1990; Dowdeswell et al., 1999).

The delivery of sediments from icebergs, meltwater, and, in particular, deforming subglacial sediment (Alley et al., 1989), is enhanced at the margins of ice streams relative to slower moving ice. The development of fast-flowing ice streams is therefore proposed to be fundamental to the growth of prograding fans and the debris flows which are their building blocks during full glacials (Dowdeswell et al., 1996a; Laberg and Vorren, 1996a, 1996b; King et al., 1996).

Between ice streams, although ice may still reach the shelf break, the rate of ice-sheet flow is one to two orders of magnitude lower (Fig. 3B). In a number of the proglacial interfan regions, very large, but infrequent, slide events have been observed (Bugge et al., 1988; Dowdeswell et al., 1996a). In some high-latitude areas, ice fails to reach the shelf break even during full glacials, and here sedimentation rates will remain low throughout a glacial-interglacial cycle (Fig. 3). The margins and deep-ocean basins beyond them are dominated by large submarine channel systems (Mienert et al., 1993).

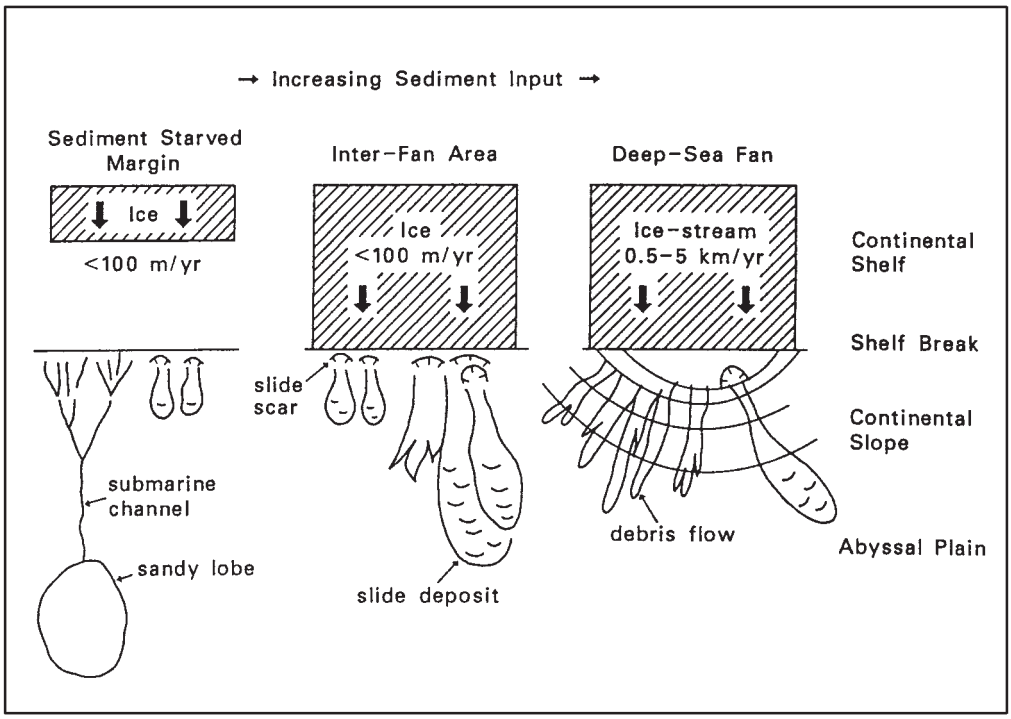

Figure 3. Conceptual model linking ice dynamics and sedimentation on glacier-influenced continental margins (adapted from Dowdeswell et al., 1996a).

In this paper we use a time-dependent numerical modeling approach to quantify the relation between ice-sheet dimensions and dynamics and the nature of the resulting sedimentation on glacier-influenced continental margins. The qualitative link between fast-flowing ice streams and fan development around the Norwegian-Greenland Sea is now widely accepted (e.g., Dowdeswell et al., 1996a; King et al., 1996; Vorren et al., 1998). Our aim is to link numerical, time-dependent predictions of ice-sheet velocity and sediment delivery with geophysical evidence on the large-scale distribution and volume of these glacier-derived sediments (cf. Hooke and Elverhøi, 1996).

NUMERICAL ICE-SHEET MODELING METHODS

Ice-Sheet Model

We couple a simple ice-sheet model with a model describing the deformation and transport of water-saturated basal sediment. The ice-sheet model is based on the continuity equation for ice (Mahaffy, 1976), where time-dependent (time = t) change in the ice thickness of a grid cell is associated with the specific net mass budget of a cell :

$$\frac{\partial h}{\partial t} = b_s(x,t) - \nabla \cdot F(h,u), \tag{1}$$

where $\nabla \cdot F(u,h)$ is the net flux of ice from a grid cell ($m^2\ yr^{-1}$) (a function of the ice thickness, h, and velocity, u, of a cell and its neighboring cells). In this study, the specific mass budget term, b_s, is related solely to the annual ice-surface accumulation. Equation 1 is solved using an explicit finite-difference technique.

The depth-averaged ice-deformation velocity, u_i ($m\ s^{-1}$), is calculated by:

$$u_i = \frac{2A\tau_b^n H}{n+2}, \tag{2a}$$

where

$$\tau_b^n = \rho_i g h \sin(\alpha). \tag{2b}$$

Here n is the flow-law exponent (equal here to 3), τ_b is basal shear stress (Pa), ρ_i is ice density (870 kg m^{-3}), α is ice-sheet surface slope, and g is acceleration due to gravity (9.81 m s^{-2}) (Paterson, 1994). The mean ice temperature of a cell is set at –10 °C, a temperature often used in isothermal ice-sheet models to determine the flow-law parameter A (5.3×10^{-15} $kPa^{-3}\ s^{-1}$; Payne et al., 1989; Arnold and Sharp, 1992). As the ice-sheet model runs, the topographic grid is continually adjusted to account for ice loading of the crust through a glacial cycle after the isostasy method developed in Oerlemans and van der Veen (1984).

Calculating Ice-Sheet Delivery of Sediments

The processes by which large-scale glacial sedimentation occurred over the Eurasian Arctic trough mouths during Quaternary time had the capacity to transport several thousand cubic kilometers of material within a few thousand years. We assume that the deformation and subsequent downslope transport of water-saturated basal sediment is the major mechanism by which glacial sediments are transported to the ice-sheet margin on the scale required. The model describing sediment deformation beneath an ice sheet is adapted from Alley (1990). An assumption is made that ice-stream activity in the late Weichselian Barents Sea was physically similar to that observed today in Ice Stream B, West Antarctica. This is supported by the finding that the geotechnical properties of diamictic sediments from the Bear Island trough are similar to those sampled from Ice Stream B (A. Solheim, 1995, personal commun.).

The model allows for the rapid deformation of basal till (which is coupled to till geotechnical properties and basal stresses) as a component of the total ice velocity. The velocity due to the deformation of water-saturated basal sediments, u_b ($m\ s^{-1}$), is determined by (Alley, 1990):

$$u_b = h_b K_b \frac{\left(\tau_b - \tau^*\right)}{N^2}, \tag{3}$$

where K_b is the till deformation softness (0.013 Pa s^{-1}), h_b is the deforming till thickness (m), and N is the effective pressure (Pa). The till yield strength, τ^*, is:

$$\tau^* = N\tan(\phi) + C \tag{4}$$

(Alley et al., 1989; Boulton and Hindmarsh, 1987), where C is the till cohesion coefficient (4000 Pa), and $\tan(\phi)$ is a dimensionless glacier-bed friction parameter (0.2) (Alley, 1990). The total velocity, u, is the sum of the sediment deformation, internal ice deformation, and any contribution from basal sliding.

The bed-deformation process assumes that there is no change in the effective pressure, N, through the deforming till thickness, h_b. Neither ploughing nor discrete shearing of the till is accounted for in the bed-deformation model (Alley, 1990). As in Alley (1990), longitudinal stresses are not calculated. The generation of subglacial till is controlled by:

$$t = K_t \frac{u_b}{h_b} N, \tag{5}$$

where t is the thickness of till produced in a year and K_t is abrasion softness (3×10^{-9} m Pa^{-1}).

Beneath Ice Stream B, the thickness of the water-saturated sediments has been found through seismic reflection studies to be around 6 m (Blankenship et al., 1986, 1987). In addition, Murray (1990) modeled the deforming thickness of subglacial till, assuming that it could be described as a Mohr-Coulomb material, and found that typical deforming thicknesses, away from the ice margin, were <6 m. Because the sediment thickness in some areas of the Barents Sea is much greater than this (e.g., Elverhøi and Solheim, 1983; Vorren et al., 1990), allowance should be made for the deforming thickness within a large column of sediments. This study assumes that a sediment thickness of 6 m is large enough to permit deformation at the top of the till column and zero deformation at the base (6 m from the top). However, field observations at the base of Icelandic glaciers suggest that the active deforming layer (where the majority of deformation takes place) is likely to be significantly less than 6 m (Boulton and Jones, 1979). We assume that the thickness over which active deformation occurs is 2 m. A sensitivity experiment that examines the relation between, first, the thickness of the deforming layer, and, second, the generation of new sediment and sediment supply to the continental margin is given later.

Ice velocity resulting from sediment deformation occurs when the sediment shears due to stresses induced by the overriding ice. Thus, a redistribution of the basal sediment will occur when the material deforms. This is modeled using a continuity equation for sediment flux, similar in form to equation 1 (Alley, 1990; MacAyeal, 1992). Just as the ice-shearing velocity observed on the ice-sheet surface must be depth corrected before it can be used to determine the flux of ice, so too does sediment deformation. As in

MacAyeal (1992), we assume that the vertically averaged horizontal velocity is half the velocity at the ice-till interface.

MODEL BOUNDARY CONDITIONS

Bedrock Elevations

It is assumed that, at ca. 30 ka, the bedrock elevation of the Eurasian High Arctic and Scandinavian region was similar to that of today, allowing the present bedrock elevation to be used to define initial model conditions. The justification for this assumption is based on sedimentary evidence from central Svalbard and Scandinavia that indicates interstadial conditions between 50 and 30 ka, when glaciers were not significantly larger than at present (e.g., Mangerud and Svendsen, 1992). The bedrock-elevation grid over which the ice sheet was constructed is composed of 46 200 square cells (220 by 210), with a width of 20 km/cell. The bed elevations were derived from a series of topographic maps and radio-echo sounding data on modern ice thickness (e.g., Dowdeswell et al., 1986, 1996b).

Sea-Level Change and Iceberg Production

During periods of ice-sheet growth, global sea level falls due to the abstraction of water from the oceans to ice sheets. We use a eustatic sea-level curve for the past 30 k.y. to determine the time-dependent change in sea level (Fairbanks, 1989). Relative sea level is then determined by summing the eustatic sea level with the isostatically adjusted bedrock elevation.

The treatment of iceberg production in our model is as follows. We assume that, at the last glacial maximum, grounded ice covered the entire Barents Shelf. In order to grow a marine-based ice sheet that occupies the entire Eurasian High Arctic, including the epicontinental Barents Sea, we do not allow iceberg calving except at the continental margin. A depth-related calving function is employed to describe the amount of ice removed from the ice-sheet margin at the shelf break. The relation used is:

$$V_c = 70.0 + 8.33h_w, \quad (6)$$

where V_c is the calving velocity (m yr^{-1}) and h_w is the water depth (m). This relation has been deduced from a statistical analysis of calving glaciers from several polar locations, including Svalbard (Pelto and Warren, 1991). Hughes (1992) outlined a depth-related physical mechanism by which glacier and ice-sheet calving might occur.

Paleoclimate Forcing

The western margin of the Eurasian High Arctic has, in relation to its high latitude, an anomalously mild climate. This is due to relatively warm southwesterly prevailing winds that transfer heat and moisture from the Norwegian-Greenland Sea (Hisdal, 1985). The temperature of the Norwegian-Greenland Sea is influenced by the meridional Norwegian Current, which transports relatively warm water from the North Atlantic. Eastward toward the Russian High Arctic, the climate becomes colder and drier (Dowdeswell, 1995). This climate gradient is illustrated by a mean annual air-temperature lapse rate of 0.6–1.0 °C/100 km across the Svalbard archipelago (Simões, 1990).

The numerical model requires climatic inputs in the form of air temperature and precipitation and their behavior with respect to geographic location and altitude. However, there is a lack of continuous proxy records from which to infer the climatic history of the Eurasian High Arctic. To construct a simple paleoclimate for the period of the last glaciation, some assumptions are made. It is first assumed that, at present, the climate of the Svalbard-Barents Sea region is similar to the altitude-precipitation relation defined as polar mix by Pelto et al. (1990), and that the climate over Scandinavia is defined as subpolar mix, following Pelto et al. (1990). Second, if the present Barents Sea moisture source was curtailed, then a more continental-type precipitation regime would exist, similar to the polar continental altitude-precipitation relation in Pelto et al. (1990). Thus, the eastern Eurasian High Arctic is described by a polar continental–type relation.

Several lines of evidence indicate that precipitation conditions similar to those of today existed over the Barents Sea during the last glaciation. In Andøya, northern Norway, dated pollen assemblages within a core from Lake Æråsvatnet suggest that relatively warm, moist climate conditions were present between ca. 24.7 and 20 ka (Vorren et al., 1988). This is supported by sedimentological and foraminiferal data from the eastern Norwegian-Greenland Sea, indicating seasonally sea-ice–free conditions at this time, and also between 19 and 17 ka (Hebbeln et al., 1994). In addition, after 16 ka, diatom records from sea-floor cores indicate that seasonally ice-free conditions were present on the eastern side of the Norwegian-Greenland Sea into Holocene time (Koç et al., 1993). In the remaining periods, due to the likely absence of a local moisture source, the polar continental accumulation function is used to describe the net surface mass balance of the ice sheet.

In the numerical model, the equilibrium line altitude is related to temperature through an adiabatic lapse rate of 5.1 °C km^{-1} (Fortuin and Oerlemans, 1990). Thus, a temperature depression of 3 °C will move the equilibrium line altitude downward by 600 m, such that it is numerically below sea level. Fleming et al. (1997), through surface energy-balance modeling of northwest Spitsbergen glaciers with a modern equilibrium line altitude of about 400 m, show that a 3 °C temperature change would shift the equilibrium line altitude below sea level, providing support for the simpler approach adopted here.

The air-temperature depression over the Barents Sea at the glacial maximum is set at 10 °C (Manabe and Bryan, 1985). Because glaciers on Svalbard were not significantly larger at 30 ka than today (Mangerud and Svendsen, 1992), an assumption is made that the temperature conditions at 30 and 10 ka (the time at which Svalbard became largely ice free, and warm waters entered the Svalbard coastal region; Salvigsen et al., 1992) were similar to those at present.

Several lines of evidence indicate the timing of onset of glacial activity within the Barents Sea. First, the preceding interstadial is thought to have lasted for longer than dated sedimentary sections within central Svalbard suggest (between 50 and 40 ka) because of the erosional unconformity that is above them (Mangerud and Svendsen, 1992). Second, ice build-up may have occurred relatively quickly within Svalbard, because the average modern equilibrium line altitude is only around 350 m (Hagen and Liestøl, 1990). An air-temperature depression of 3 °C would result in the depression of the equilibrium line below sea level and would encourage glacier margins to migrate rapidly beyond their present positions. Third, radiocarbon-dated sea-floor glacial sediment samples indicate that grounded ice existed over the lower slopes of Spitsbergenbanken in the north-west Barents Sea at 26 ka (Sættem et al., 1992; Elverhøi et al., 1993). Fourth, seasonally ice-free conditions within the eastern Norwegian-Greenland Sea at and after 27 ka (recorded in foraminifera and ice-rafted debris) provide a moisture source from which a relatively high rate of precipitation can be supplied to the Svalbard-Barents Sea area (e.g., Hebbeln et al., 1994, 1998). Therefore, the onset of large-scale glacier activity in Svalbard and the Barents Sea may have occurred both relatively late and rapidly in the last glaciation. Mangerud and Svendsen (1992) concluded that the late Weichselian glaciation of the Barents Sea began as late as 28 ka. Thus, the model begins the glacial simulation at 30 ka, when interstadial conditions relatively similar to those of today were present.

There is a clear correlation between high-latitude paleo-air temperatures (e.g., recorded in Greenland ice-core records) and indicators of global ice

volume (e.g., Barrett, 1991), such as the global sea level, carbon dioxide, and oxygen isotope curves. Because of this, the air-temperature change through time in the Svalbard-Barents Sea region can be calculated empirically by one of the three indicators of global ice volume (because the actual time function of air temperature is unknown for the Barents Sea region). Our results use the carbon dioxide forcing function, but previous experiments have shown that there is little effect on ice-sheet size by selecting either sea level or oxygen isotopic forcing functions (Siegert, 1993; Siegert and Dowdeswell, 1995).

ICE SHEETS IN THE EURASIAN ARCTIC: MODEL RESULTS

General Growth and Decay of the Eurasian High Arctic Ice Sheet

Ice growth in the model began at 27 ka, when ice began to build up over Scandinavia, Svalbard, and the Russian Arctic islands. Ice then flowed from these terrestrial locations into the shallow Barents and Kara Seas, associated with the suppression of iceberg production in the model. The rate of accumulation was relatively high ca. 25 ka, and ice growth was rapid. As temperatures reached their minimum values for the last full glacial, the rates of ice accumulation and change in ice volume decreased (Fig. 4, A and B).

By 16 ka, the ice sheet had reached its maximum volume and the process of iceberg calving is allowed in the model to occur over the continental shelf region. At this time global sea level, having reached a minimum of –120 m at 18 ka, was beginning to rise, causing an increase in depth-related iceberg calving at the marine margins of the ice sheet. After 16 ka, a series of iceberg-calving events, linked to the presence of ice margins in deep water, caused the rapid collapse of the marine portions of the ice sheet. For example, ca. 14 ka, a short-lived (200 yr) calving event (Fig. 4C), which is characterized by a maximum rate of calving of 2000 $km^3\ yr^{-1}$, caused a 30% decay in ice-sheet volume (Fig. 4A). This ice decay was concentrated around the deep bathymetric troughs (to 500 m) in the Eurasian High Arctic shelves. Subsequent, less marked calving events caused ice decay in shallower regions of the Barents and Kara Seas. By 11 ka, as air temperatures returned to their modern values, the equilibrium line altitude rose above the margins of the terrestrial portions of the ice sheet and large-scale surface melting of the ice sheet took place, as indicated by negative accumulation in Figure 4B. Thus, by 10 ka the Eurasian ice sheet had largely decayed, except for small ice caps located on Scandinavia and the high Arctic archipelagos.

Ice-Surface Elevation and Thickness

Ice was able to build up over the Barents and Kara Seas relatively rapidly because, in the numerical model, iceberg calving over the continental shelf did not take place during ice-sheet growth. By 25 ka, ice domes were predicted to develop over Scandinavia, Svalbard, and Novaya Zemlya (Fig. 5A). The ice-thickness distribution was ~1200 m of ice over Scandinavia, ~800 m over the Barents Sea, and ~400 m over the Kara Sea (Fig. 6A). During the subsequent 5 k.y. a rapid increase in ice thickness and, therefore, in the surface elevation of the ice sheet, occurred over Scandinavia such that by 20 ka the Eurasian High Arctic ice sheet was dominated by a 2.5-km-thick dome over Scandinavia (Fig. 6B). Ice flowed from this dome into the southern Barents Sea, where 1200 m of ice was grounded on the sea floor. A small ice dome over Novaya Zemlya (Fig. 5B) acted as an ice divide between the Barents and Kara Seas. The morphology of the ice surface was controlled to an extent by fast-flowing ice streams located in bathymetric troughs within the continental shelves, which drained ice from the central regions.

The ice sheet reached a maximum volume by 16 ka (Fig. 4A), when a 3.2-km-thick ice dome existed over Scandinavia (Fig. 6C). Ice from this dome flowed over the southern Barents Sea and, in contrast to the situation

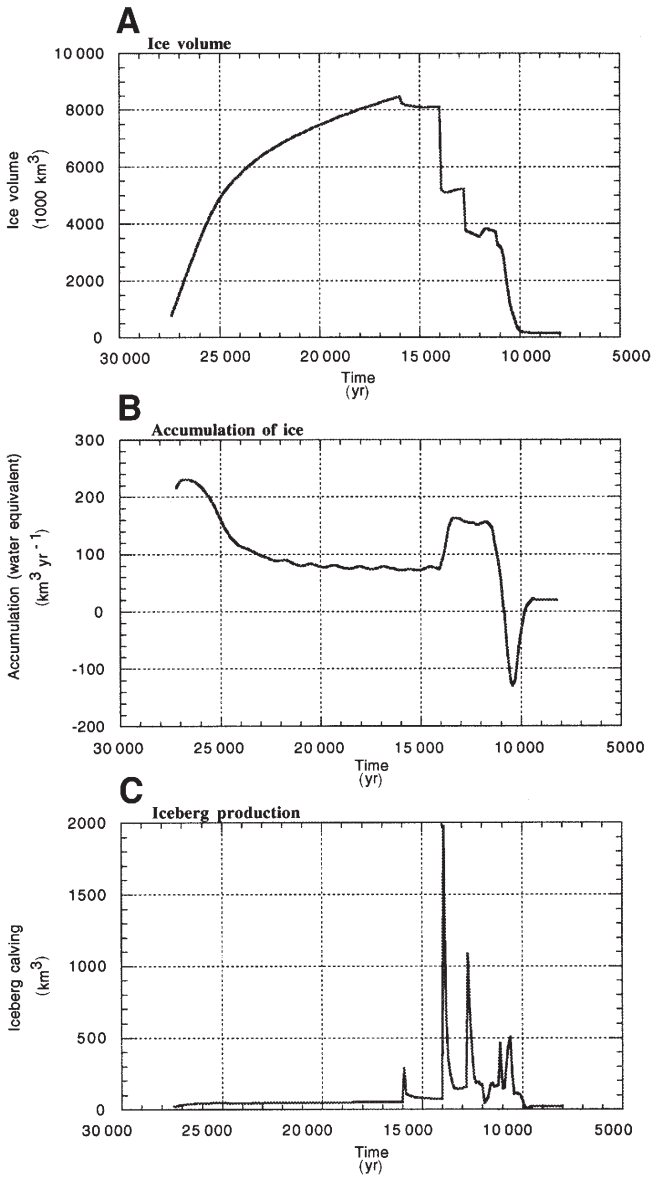

Figure 4. Changes in predicted ice-sheet parameters over the past 30 k.y. for the entire model grid (Fig. 1), including both the Barents-Kara and Scandinavian ice sheets. (A) Ice-sheet volume. (B) Accumulation of ice. (C) Iceberg production.

at 20 ka, also flowed over Novaya Zemlya (Fig. 5C). Ice streams continued to drain ice from the central regions of the ice sheet (Fig. 7). After 15 ka, rising sea level caused water deepening and the marine portions of the ice sheet underwent increased buoyancy. Because, in the model, iceberg calving is related linearly to water depth, a series of large-scale iceberg calving events after 15 ka resulted in the break-up of the marine-based ice sheet (Fig. 4C).

Rising temperatures after 14 ka also caused a relatively large increase in the rate of ice accumulation due to increased moisture availability (Fig. 4B). However, this was negated quickly by a general increase in iceberg calving that caused net loss of ice (Fig. 4C) and by surface ablation from about 12 ka (Fig. 4B). By 10 ka, the ice sheet had all but decayed (Figs. 5D and 6D). The only remaining ice was a 1-km-thick ice cap over Scandinavia.

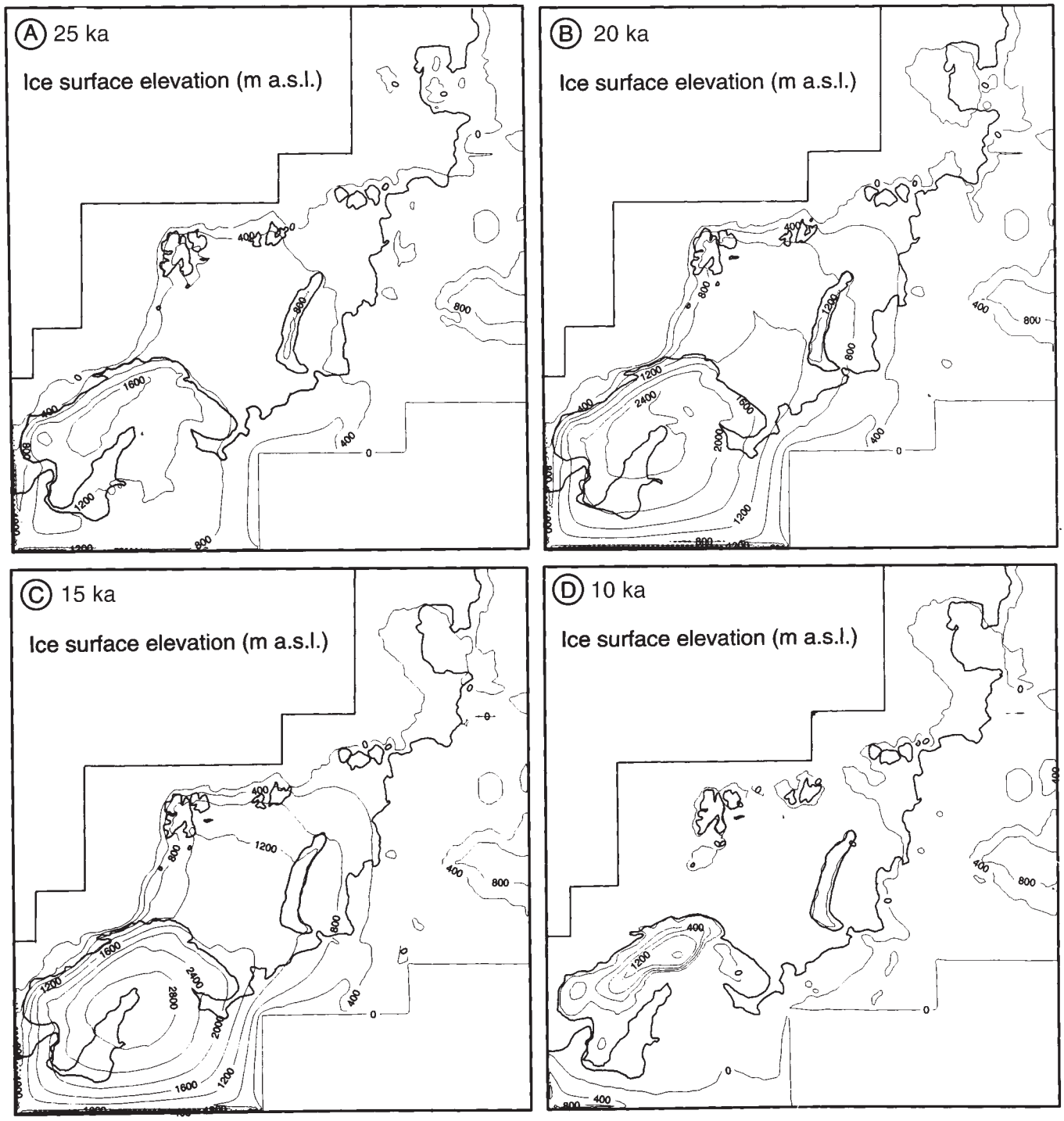

Figure 5. Ice-sheet extent and surface elevation at four time slices during the past 30 k.y. (A) 25 ka. (B) 20 ka. (C) 15 ka. (D) 10 ka. The Eurasian Arctic coastline is provided as an aid to location.

Ice Velocities and Ice-Stream Development

The model predicts that, shortly after the commencement of glaciation on the Barents Shelf, ice streams within bathymetric troughs were activated. The largest of these ice streams were located within the Bear Island trough, Storfjorden trough, Franz-Victoria trough, and the St. Anna trough (Fig. 1). The morphology of the Barents Shelf thus has an influence on the dynamics of the ice sheet (Siegert and Dowdeswell, 1996). Ice streams drain the central ice-sheet regions and, if their beds are actively deforming, also result in the transport of sediment at the glacier base to the ice-sheet margin.

By 27 ka, the Bear Island trough was filled by a fast-flowing ice stream. This ice stream was active for 13 k.y. By 25 ka, the Bear Island trough ice

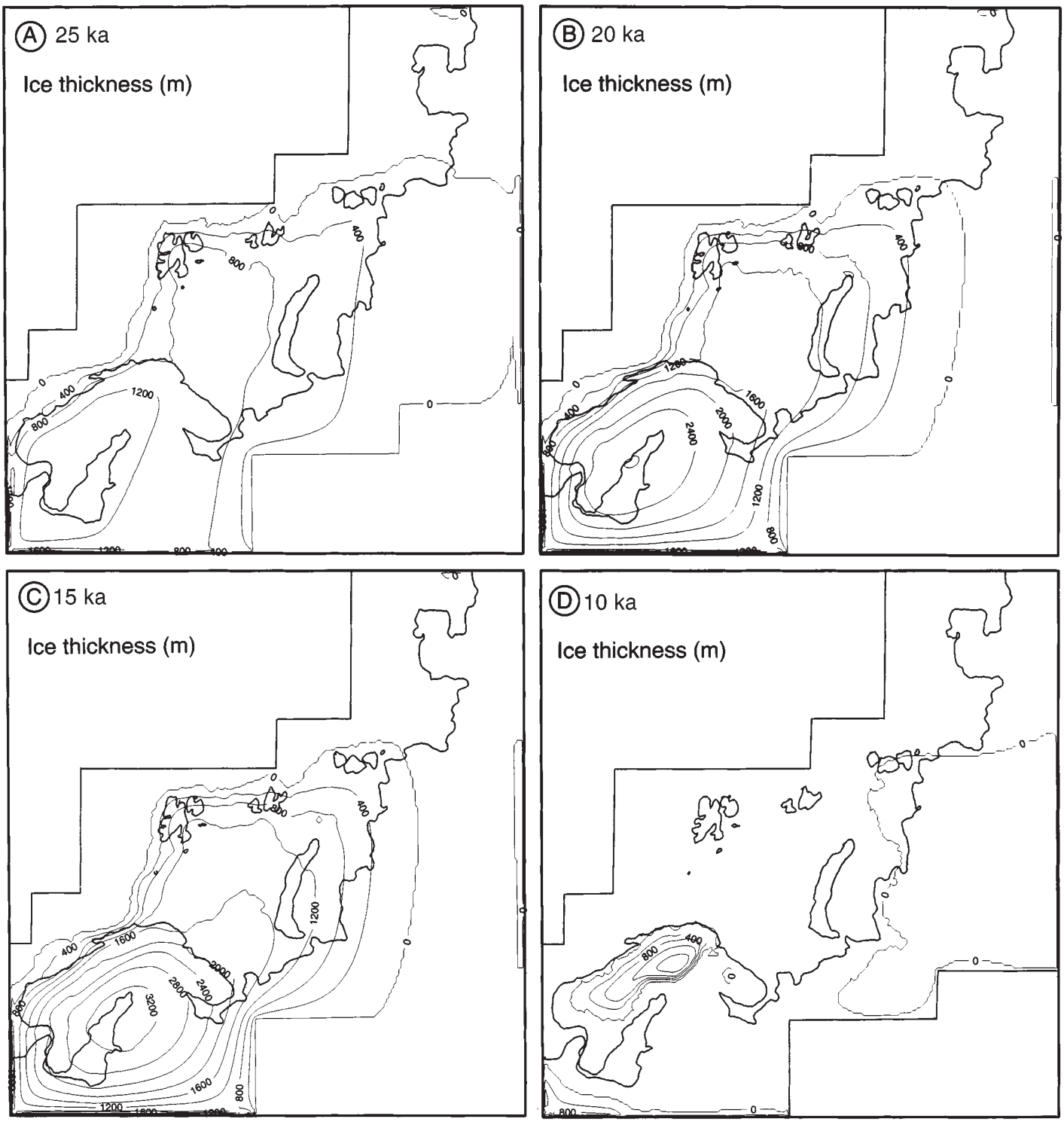

Figure 6. Ice-sheet thickness at four time slices during the past 30 k.y. (A) 25 ka. (B) 20 ka. (C) 15 ka. (D) 10 ka. The Eurasian Arctic coastline is provided as an aid to location.

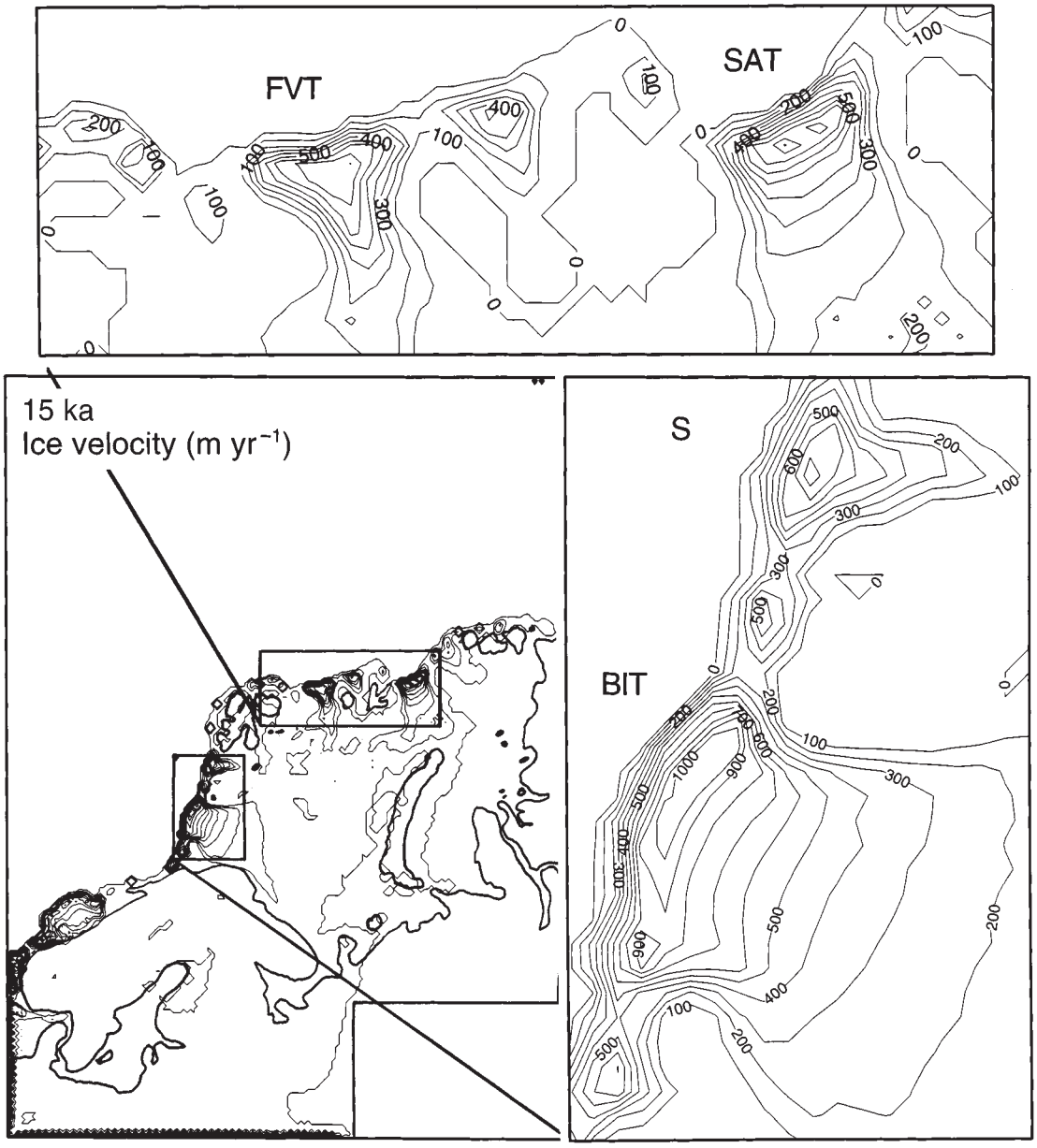

Figure 7. Ice-sheet surface velocity at 15 ka (contour interval 100 m yr^{-1}). The western and northern continental margins are enlarged within insets. The Eurasian Arctic coastline is provided as an aid to location. BIT—Bear Island trough, S—Storfjorden trough, SAT—St. Anna trough, FVT— Franz-Victoria trough.

stream had a maximum velocity ~1000 m yr^{-1} along its 350 km seaward margin. This ice stream was more than twice as wide as any other within the ice sheet and thus acted as a significant focus for ice flux. The model predicts that ca. 25 ka the Bear Island trough ice stream drained 24 km^3 yr^{-1} of ice (Table 2). This value represents about half the total volume of icebergs produced along the continental margin at this time. The ice velocity of the Bear Island trough ice stream remained relatively constant throughout the subsequent 10 k.y. (Table 1). At 15 ka, ice-stream velocity was more than 800 m yr^{-1} (Fig. 7) and ice flux at the margin was 32 km^3 yr^{-1}, representing 40% of ice lost through iceberg calving along the seaward edge of the Eurasian ice sheet (Table 2). By 13 ka, ice decay in the deeper regions of the Barents Shelf terminated ice-stream activity over the Bear Island trough.

The ice stream within the Storfjorden trough was present for 15 k.y. between 27 and 12 ka. At 15 ka, flux through the ice stream reached a predicted maximum of 7.2 km^3 yr^{-1} (Table 2) and the ice velocity was ~800 m yr^{-1} (Fig. 7). As sea-level rise occurred after 15 ka, the effective pressure beneath the ice stream decreased and, as a consequence, ice velocity increased. Calving of the ice sheet over relatively deeper regions of the continental shelf did not affect the Storfjorden trough area until 12 ka.

On the northern, Arctic Ocean margin of the Eurasian shelf, major ice streams formed over the St. Anna and Franz-Victoria troughs by 25 ka. Although initially the volume of ice drained by the St. Anna ice stream was similar to the Storfjorden ice stream, by 15 ka the St. Anna trough ice stream had a flux of ice equal to about half that in the Bear Island trough (Table 2).

TABLE 2. VOLUME OF ICE DRAINED BY MAJOR EURASIAN HIGH ARCTIC ICE STREAMS AT THREE TIMES DURING THE LAST GLACIATION

Ice stream	Ice flux at 25 ka $km^3\ yr^{-1}$	Ice flux at 20 ka $km^3\ yr^{-1}$	Ice flux at 15 ka $km^3\ yr^{-1}$
Bear Island Trough	24.0	27.0	32.0
Storfjorden	4.8	4.8	7.2
St. Anna Trough	6.2	6.2	15.0
Subtotal	**35.0**	**38.0**	**54.2**
Total ice calved	*47.0*	*50.0*	*80.0*

Notes: Table provides the sum of ice volume drained by these ice streams and the total volume of ice calved by the Eurasian Ice Sheet. Locations are given in Figure 1.

This increased flux was associated with the growth of the drainage basin supplying ice to the St. Anna trough, as a result of the reduced importance of Novaya Zemlya as an ice divide (Fig. 5, B and C). Thus, the St. Anna trough ice stream was the second largest within the Barents-Kara Sea during the last glacial. The ice velocity at 15 ka was ~800 m yr^{-1} (Fig. 7). Ice decay within the St. Anna trough occurred relatively late, such that the ice stream was active until 11 ka. This is because a significant ice mass existed at that time over the northern Barents Sea and fed ice into the St. Anna trough. Polyak et al. (1997) inferred a similar history from dated cores, with stepwise retreat of ice from the St. Anna trough and final deglaciation about 10 ka.

To summarize, modeled ice-stream evolution within the late Weichselian Barents Sea is characterized by: (1) ice streams located within bathymetric troughs; (2) onset of activity ca. 27 ka; (3) a relatively steady flux of ice transported through the troughs from 26 to 15 ka; (4) an increase in ice velocities after 15 ka and, therefore, in the flux of ice transported through the ice streams; and (5) decay of the ice sheet after 13 ka. The largest ice stream in the Eurasian High Arctic, by a factor of at least two, was that in the Bear Island trough (Fig. 7, Table 2).

SENSITIVITY OF THE ICE SHEET TO VARIATIONS IN MODEL INPUTS

The paleoenvironmental conditions used as inputs to the model are limited for the Eurasian Arctic during late Weichselian time. Although we note that the actual paleoenvironment may have differed from that used in our experiments, we suggest that it is unlikely that this variation would be more than about 20%. Several experiments were undertaken to examine the sensitivity of the ice sheet to changes in individual environmental inputs (Fig. 8). The ice-sheet volume for 15 ka was recorded (8 110 000 km^3) and compared with the volume determined from what we regard as the most likely inputs. In addition, the time-dependent variation in ice volume was also recorded (Fig. 8). Inputs controlling directly the mass balance of the ice sheet (i.e., rates of accumulation and iceberg calving) and the maximum sea-level depression were adjusted by a maximum of 20% of their original value. Of these three exercises, the ice sheet was found to be most sensitive to alterations in accumulation, which produced a change in ice-sheet volume to 9 850 000–6 500 000 km^3. The iceberg-calving experiment yielded an ice volume of 8 100 000–8 120 000 km^3, whereas the sea-level test showed a variation between 7 360 000 and 8 260 000 km^3.

Other sensitivity experiments involving large percentage changes (20%) in the surface air temperature (and hence the equilibrium line altitude) produced relatively small changes in ice volume (7 450 000 km^3 and 7 590 000 km^3) (Fig. 8). Both these ice volumes are lower than the prediction of 8 110 000 km^3 based on most likely inputs, because net accumulation of ice becomes lower with both higher and lower temperatures. Furthermore, significant changes (10%) in the dynamics of the ice-sheet model (i.e., in parameters involving ice temperature, basal sliding, and deforming sediment relations) produced smaller ice-volume variations than the sea-level depression experiment. In conclusion, although the ice-sheet dimensions are most sensitive to alterations in imposed environmental conditions, relatively large (20%) changes in the inputs of accumulation, iceberg calving, and sea level did not greatly affect the results presented here.

COMPARISON OF THE LATE WEICHSELIAN ICE SHEET WITH OTHER RECENT MODELS

By modeling the response of the Earth's crust to glacial loading and unloading through time, the theoretical mass of ice required to form raised shorelines of known age can be established. Lambeck (1995, 1996) used such a numerical technique to determine the possible ice thickness and extent of the Barents Sea ice sheet during late Weichselian time, by allowing his model to be forced by the uplift pattern observed in the raised beach record around Svalbard (e.g., Forman, 1990; Forman et al., 1995). Conclusions drawn from Lambeck's modeling investigation include the following: (1) the maximum ice thickness, centered over easternmost Svalbard, was 1500 to 2000 m (Lambeck 1995); (2) the ice sheet extended to the shelf break west of Svalbard and along the northern Barents margin; (3) ice-sheet decay began ca. 15 ka, but was relatively slow until 13 ka; (4) by 12 ka the ice sheet was limited to the northern regions of the Barents Sea (a continuous ice sheet from Svalbard to Franz Josef Land); and (5) by 10 ka, the ice sheet had essentially decayed. The ice thickness over the nearby Kara Sea was modeled to be relatively thin, compared with previous reconstructions where a thicker ice load was located over Novaya Zemlya (e.g., Grosswald and Hughes, 1995).

Our ice-sheet model compares relatively closely with that determined by Lambeck (1995), in that (1) maximum ice thickness in the Barents Sea was >1400 m (Fig. 6B); (2) the maximum ice thickness over the Kara Sea was <1200 m (Fig. 6C); (3) ice extended to the shelf break along the western and northern continental margins of Eurasia (Figs. 5 and 6); and (4) ice-sheet decay affected the marine portions of the ice sheet after 15 ka (Fig. 4), leaving a northern ice mass between Svalbard and Franz Josef Land that decayed after 13 ka.

MODELING SEDIMENT DELIVERY TO THE EURASIAN ARCTIC CONTINENTAL MARGINS

In our model it is assumed that ice-stream activity in bathymetric troughs within the Eurasian shelves is associated with a deforming water-saturated sediment layer beneath the ice (Alley, 1990). Due to the process of deformation, this sediment is transported to the ice-sheet margin. Thus, when ice is at the continental shelf break at the glacial maximum (Fig. 5C), glacially derived sediment accumulates at the mouths of bathymetric troughs. The model calculates: (1) the spatial distribution of subglacial sediment over the Eurasian High Arctic; (2) the volume of sediment that accumulates at the

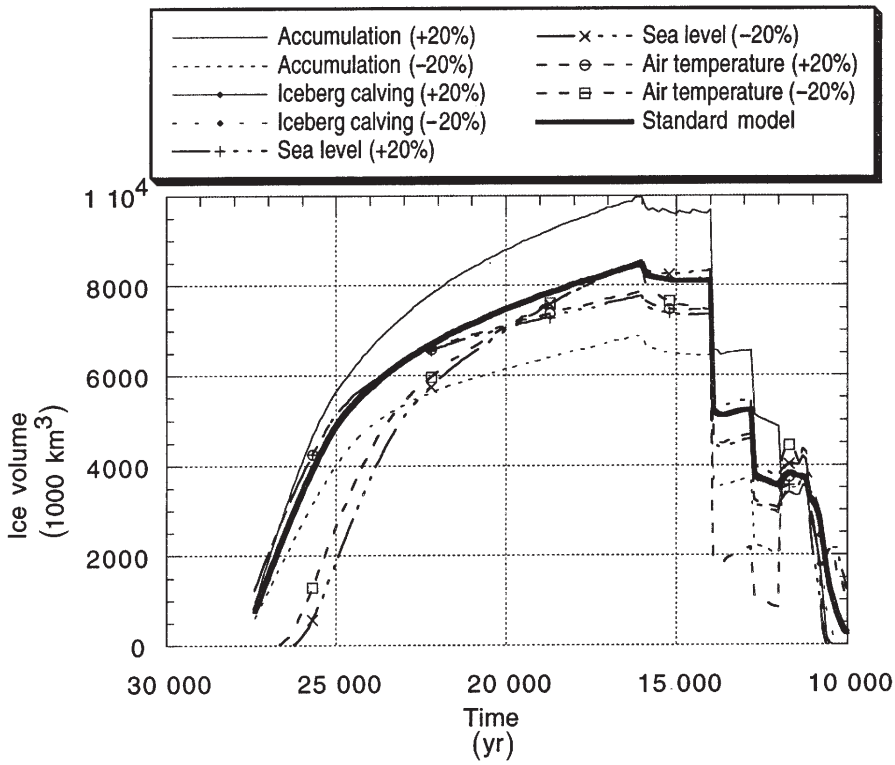

Figure 8. The time-dependent change in ice-sheet volume for a variety of ice-sheet environmental inputs. The graph indicates ice-sheet sensitivity to the late Weichselian environment.

shelf edge at the mouths of bathymetric troughs; and (3) time-dependent variations in the rate of sediment supply to the continental margin. It does not account for gravity-driven processes that transport sediment from the continental shelf edge to the large fan systems on the slope. However, we assume that sediment supplied to the margin due to subglacial deformation is distributed down the fans by processes such as debris flows (e.g., Dowdeswell et al., 1996a; Elverhøi et al., 1997; Vorren et al., 1998).

Our numerical model results are now compared with a number of geophysically derived data sets concerning sedimentation rates and sediment volumes associated with trough mouth fans during the last glacial advance.

Distribution of Subglacial Sediments

The model predicts that, by 25 ka, ~10 m of sediment had accumulated within the deeper bathymetric regions. After 7 k.y. of glacial activity, the build-up of sediment at the continental margin becomes noticeable in that >20 m of sediment had collected at the mouth of the Bear Island trough. Ice-stream activity after 20 ka produced significant thicknesses of sediment over the bathymetric troughs and large volumes of sediment at the mouths of these troughs. For example, at 15 ka, 24 m of sediment covered the floor of the Bear Island trough, while >60 m of sediment had accumulated at the trough mouth (Fig. 9A). Similarly, over the Storfjorden trough, 6 m of sediment had accumulated over the trough floor, and >20 m had collected at the shelf break at 15 ka (Fig. 9A). The St. Anna trough had ~10 m of sediment within it, and >24 m in thickness at the shelf break (Fig. 9A).

The sediment distribution after 15 ka was influenced by (1) enhanced ice-stream activity, which caused an increase in sediment delivery, and (2) ice-sheet decay, which affected the location of the ice margin and, hence, the location at which sediment build-up occurred. Because of this, by 10 ka large volumes (on the order of hundreds to thousands of cubic kilometers) of sediment had accumulated at the trough mouths (Fig. 9B). The bathymetric troughs were covered by several tens of meters of sediments. The model also predicts that, between 15 and 10 ka, a significant volume of sediment was deposited around the 400 m contour in the western Barents Sea. This represents a slowing or stillstand in the ice-sheet margin during deglaciation, which appears similar to the pattern of ice-marginal sediments reported from geophysical investigations to have been deposited in the northwestern Barents Sea during ice-sheet decay (Elverhøi and Solheim, 1983).

Volume of Sediment Delivered to Trough Mouths

We establish the volume of sediment transported to the trough mouths by selecting regions over which the time-dependent increase in sediment volume can be monitored. Three regions were identified in the model, at the mouths of the Bear Island, Storfjorden, and St. Anna troughs (Fig. 1). It is these sediments that are transported downslope to produce long-term build-up and progradation during successive glacial cycles (Fig. 2). Our calculations of sediment supply to the margin are compared directly with geophysical measurements of late Weichselian sediment volume. About 4200 km^3 of sediment was deposited over the Bear Island fan, while 700 km^3 accumulated over the Storfjorden trough mouth fan (Laberg and Vorren, 1996a, 1996b).

Model results show that sediment build-up began after 27 ka (Fig. 10). A steady rate of sediment supply to the fans occurred until 16 ka. After this, rising sea level induced increased speeds within the ice streams that increased the rate of sediment delivery to the trough mouths (Fig. 10A). The rate of sediment supply was reduced after 14 ka as ice-sheet decay began.

We calculate that 4600 km^3 of sediment was delivered to the Bear Island

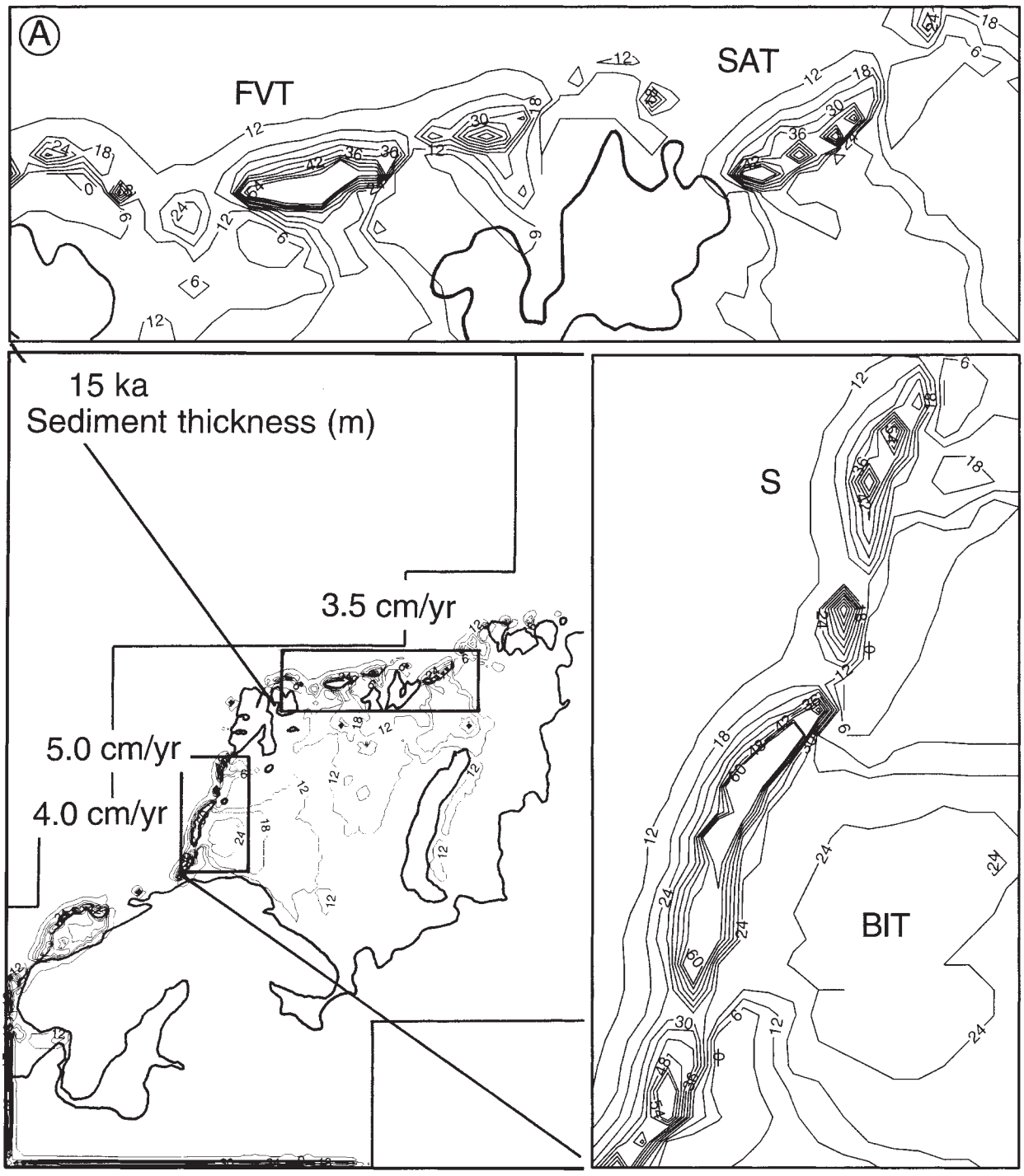

Figure 9. Thickness of sediment delivered to the ice-sheet margin, with the northern and western margins enlarged, at (A) 15 ka and (B) 10 ka. The Eurasian Arctic coastline is provided as an aid to location. The rates (in cm/yr) shown on the diagram refer to mean sediment delivery to the ice margin for the Bear Island trough (BIT), the Storfjorden trough (S), and the St. Anna trough (SAT) for each period. FVT—Franz-Victoria trough.

fan between 27 and 12 ka, and 900 km^3 of sediment built up over the Storfjorden fan between 27 and 11 ka (Fig. 10A). Our model results compare favorably with the volumes of sediment over the fans measured through geophysical investigations. The model also indicates that 2200 km^3 of sediment was delivered to the St. Anna fan (Fig. 10), an area on the Arctic Ocean margin of Eurasia where few geophysical data have been collected.

Rates of Sediment Delivery to the Continental Margin

The rate of sediment build-up across two transects, located over the western and northern continental margins of the Eurasian High Arctic (Fig. 1), was recorded by the model for 25, 20, and 15 ka (Fig. 11). The major bathymetric troughs, and therefore ice streams, on both the western and northern

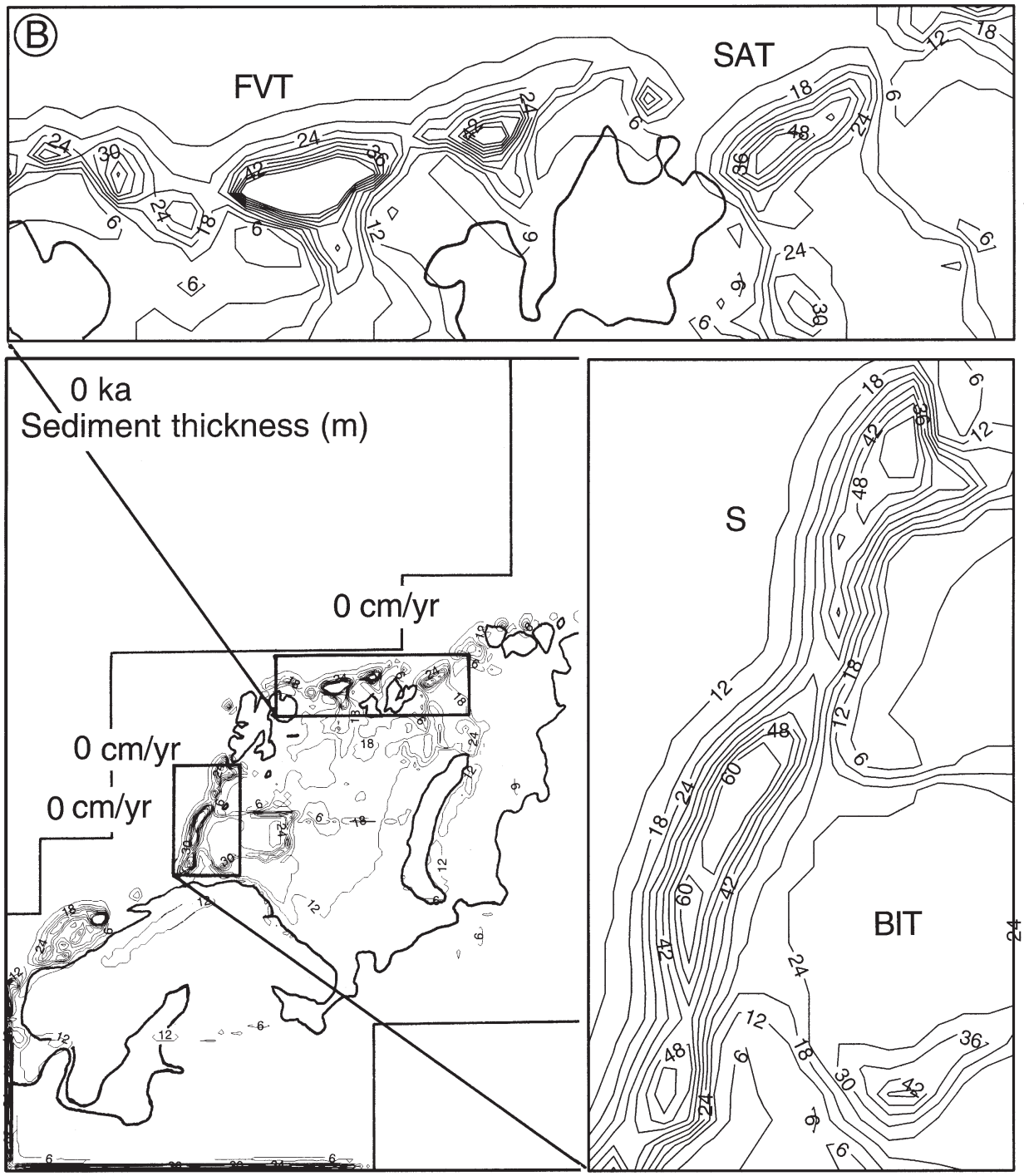

Figure 9. (*Continued*).

margins of the Barents-Kara shelf are included in the transects. The sediment volume supplied to the mouths of the Bear Island trough, the Storfjorden trough in the west, and the St. Anna and Franz-Victoria troughs to the north (Fig. 10) represent the mean values of sedimentation rates across the respective trough mouths in Figure 11.

These sedimentation rates represent the sediment supply along a 20-km-wide, ~1000-km-long transect. Thus, the rates appear to be high when compared with rates of sediment build-up over the fan system. However, because we assume that sediment delivered to the continental margin will be dispersed over the fans, we can determine the predicted rate of build-up of each fan from our calculations of sediment supply to the margins by accounting for the respective areas over which deposition takes place.

Bear Island Trough. The area over which sediment delivery to the Bear Island trough mouth was recorded was a series of 20-km-wide grid cells along 350 km of the ice margin. The rate of sediment supply at 25 ka averaged 2.5 cm yr^{-1} (Fig. 11A). As a mean over the fan area (280 000 km^2,

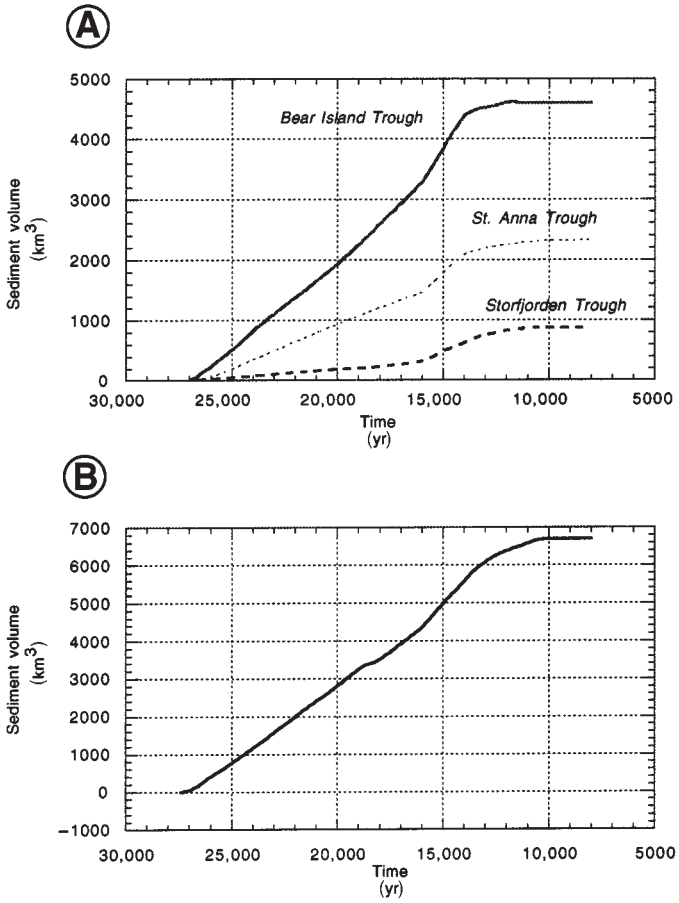

Figure 10. (A) Model predictions of the build-up of sediment volume through the past 30 k.y. for three areas of major fan deposition around the Barents-Kara ice sheet. Sediment volumes are determined by calculating the amount of material within a predefined region of the shelf (shown as boxes in Fig. 1). (B) The volume of sediment that is removed from beneath the ice sheet over 30 k.y.

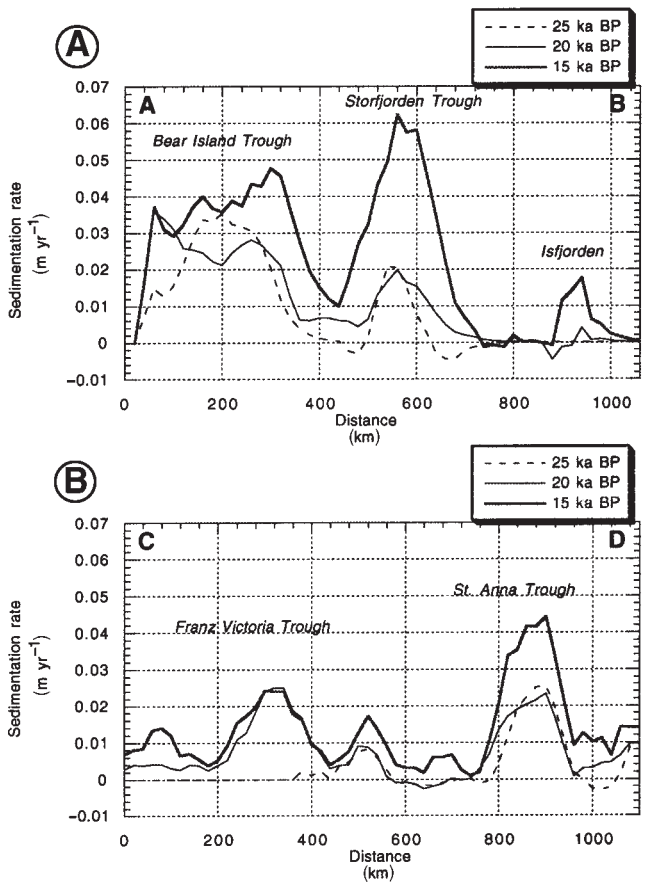

Figure 11. The rate of model-predicted sediment delivery along transects across the western and northern Eurasian continental margin (located in Fig. 1). (A) The Barents Sea–Svalbard margin (A–B). (B) The Arctic Ocean margin between Svalbard and Severnaya Zemlya (C–D). The sedimentation rate is given for time slices at 25, 20, and 15 k.y.

Laberg and Vorren, 1996a), this is a sedimentation rate of 0.08 cm yr^{-1}. By 20 ka, the rate had increased to 2.8 cm yr^{-1} (or 0.09 cm yr^{-1} over the fan) and by 15 ka had increased to 4.0 cm yr^{-1} (or 0.13 cm yr^{-1} over the fan). The average rate of late Weichselian full-glacial sedimentation for the Bear Island fan, based on dated core material (Laberg and Vorren, 1996a), is 0.124 cm yr^{-1} (Table 1). Our results concerning the rate of sediment supply to the continental margin at the mouth of the Bear Island trough are thus in broad agreement with information from these geological measurements.

Storfjorden Trough. The time-dependent evolution of sediment supply to the mouth of the Storfjorden trough changes markedly through the period after 25 ka (Figs. 10A and 11A). Between 25 and 20 ka, the average rate of sediment supplied to the margin was predicted to be 1.0 cm yr^{-1} across the 180-km-wide seaward margin of one grid cell. This build-up rate corresponds with the measured sedimentation rate, 0.1 cm yr^{-1}, over the entire fan (40 000 km^2; Laberg and Vorren, 1996b). However, at 15 ka, the rate of sediment supply to the continental margin had risen to 5.0 cm yr^{-1} (or ~0.5 cm yr^{-1} over the entire fan region). Averaged over the full 15 k.y. of sediment build-up, the model calculates that the rate of sedimentation to the Storfjorden margin was a mean of 2.3 cm yr^{-1} (or 0.23 cm yr^{-1} over the fan). The geophysically derived sedimentation rate over the Storfjorden fan during the late Weichselian glacial advance is 0.172 cm yr^{-1} (Laberg and Vorren, 1996b). Thus, our model of sediment build-up and supply is in general agreement with observations.

Northern Continental Margin of the Eurasian High Arctic. Given the success in matching our model predictions with geophysical measurements of the rate of sediment delivery to the western continental margin of Arctic Eurasia, we now predict the rate of sediment supply to trough mouths on the Arctic Ocean margin, where few geophysical data have been gathered. The model predicts an average rate of sediment supply to the St. Anna trough mouth of 1.5 cm yr^{-1} at 25 and 20 ka (Fig. 11B). However, by 15 ka, the rate of sediment supply had increased to 3.5 cm yr^{-1}. The model also calculates that 2200 km^3 of sediment was delivered to the fan during the last full glacial. It appears likely from these results that, if the late Weichselian glacial advance was typical of that to the west, the fan at the mouth of St. Anna trough is significantly larger than the Storfjorden fan.

Several other bathymetric troughs exist along the northern margin of the Eurasian continental shelf (Fig. 1). The numerical model suggests that ice streams were located within these troughs (Fig. 7) during late Weichselian

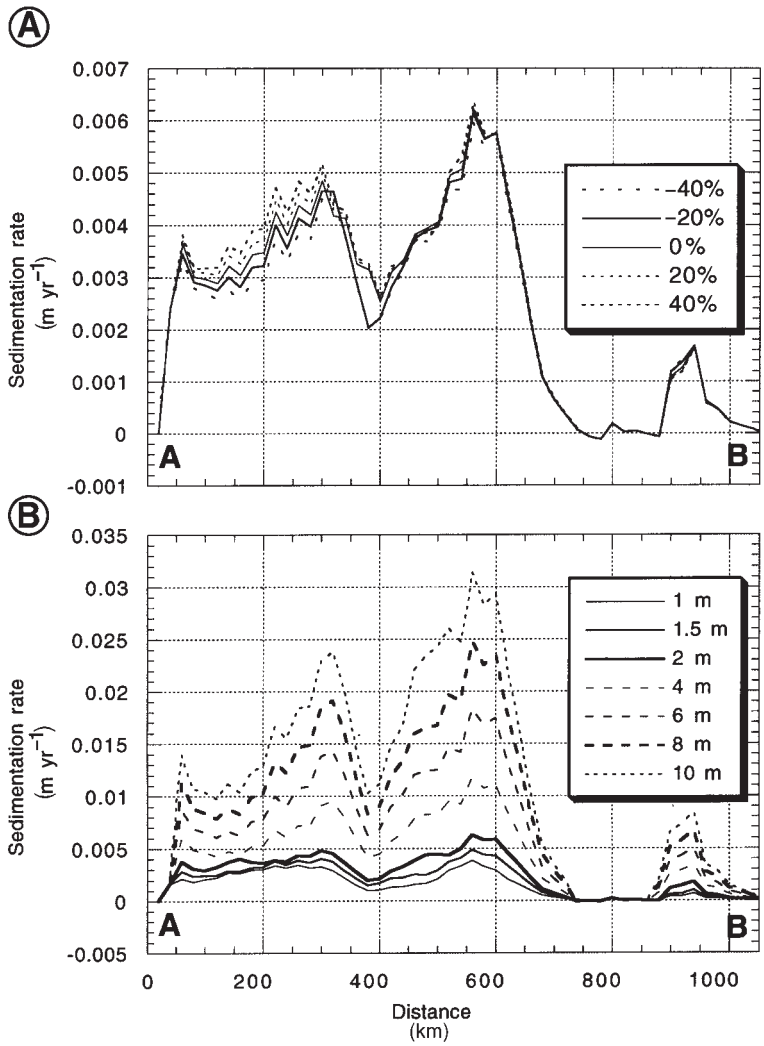

Figure 12. Sensitivity of the rate of model-predicted sediment delivery along transect A–B (located in Fig. 1) for a time slice at 15 ka. (A) Variation in generation of sediment. (B) Variation in thickness of the deforming layer.

time and therefore, under our modeling assumptions, sediment was transported to the continental margin at the mouth of the Franz-Victoria trough at a rate of 1.5 cm yr^{-1} between about 20 and 15 ka (Figs. 9 and 11B).

Sensitivity of Results to Variations in the Sediment Model

Two series of examinations were performed to establish the sensitivity of results to changes in the sediment deformation model. The first investigated the effect of changes in the generation of subglacial till (equation 5) on the rate of sediment supply to the continental margin. The second analyzed the response of model results to variations in the thickness of the deforming sediment layer (h_b; equation 3). Relatively large percentage changes (40%) to the amount of sediment generated beneath the ice sheet did not affect greatly the rate of transport of basal sediment to the continental margin (Fig. 12A). Thus, our model of subglacial sediment delivery to trough mouth fans is insensitive to the generation of new sediment, if a relatively thin veneer of sediment exists across the Barents Shelf (as is the case at present). Our second sensitivity test revealed that, by changing the thickness of the deforming sediment layer, the rate of supply of sediments to the Barents margin was modified (Fig. 12B). In addition, our test showed that, by changing the thickness of the deforming layer, the volume of sediment supplied to trough mouth fans is affected (Table 3). However, our sensitivity results indicate that extremely large alterations (>200%) to the deforming thickness were required to force model results to be incompatible with geological evidence of late Weichselian sediment volume over fans. Because of this we conclude that our model of sediment supply to the continental margin is not adversely affected by significant variation (50%) in a deforming sediment thickness of 2 m.

SUMMARY AND CONCLUSIONS

Seismic reflection data and GLORIA and SeaMARC II side-scan sonar imagery have revealed that large sedimentary fans at the mouths of Eurasian continental shelf troughs are characterized by a series of stacked debris flows that distribute sediment downslope (Fig. 2) (e.g., Vogt et al., 1993; Dowdeswell et al., 1996a; Vorren et al., 1998). The origin of the material is glacial and dates from times when large ice sheets occupied the Eurasian High Arctic. We have used a numerical ice-sheet model, which accounts for subglacial deformation and transport of water-saturated sediment, to deter-

TABLE 3. SENSITIVITY OF THE VOLUME OF MODEL-PREDICTED SEDIMENT DELIVERED TO THE BEAR ISLAND, STORFJORDEN, AND ST. ANNA TROUGH MOUTH FANS TO VARIATION IN THICKNESS OF THE SUBGLACIAL DEFORMING SEDIMENT LAYER

Thickness of active layer (m)	Bear Island Trough (km^3)	Storfjorden Trough (km^3)	St. Anna Trough (km^3)
1	2821	294	1128
1.5	3588	349	1507
2	**3840**	**480**	**1780**
4	4730	890	2020
6	5890	1270	2600
8	7280	1700	3370
10	8780	2140	4230

Notes: Sediment volumes are for the period 30 to 10 ka. The bold text denotes results from main model run.

mine the late Weichselian glacial conditions required to deliver sediment to the continental margins. The model inputs were (1) known bathymetry and (2) late Weichselian environmental conditions. A series of sensitivity experiments indicated that significant adjustments to model environmental inputs do not adversely affect model results (Figs. 8 and 12). On the western Barents Sea margin, model predictions were tested against seismically derived measurements of sediment volumes and dated cores for which the rate of sedimentation has been established (Table 1). Our model results are close to the observed values for both measured volumes and sedimentation rates. On the basis of this good match, the numerical model was also used to predict sediment delivery patterns and rates to the Arctic Ocean continental margin north of the Barents and Kara Seas, where little geophysical work has been undertaken.

Our modeling results predict that (Figs. 6 and 7): (1) the most recent glaciation of the Eurasian High Arctic occurred after 28 ka, and that ice streams within bathymetric troughs were active by ca. 25 ka; (2) the maximum ice thickness over the Barents Sea exceeded 1400 m; (3) the ice thickness over the Kara Sea was <1200 m; (4) ice extended to the shelf break along the both the western Barents Sea margin and the Arctic Ocean margin north of the Barents and Kara Seas; (5) ice-sheet decay affected the marine portions of the ice sheet after 15 ka, leaving a northern ice mass between Svalbard and Franz Josef Land that decayed after 13 ka; and (6) ice streams draining the Barents and Kara Seas were present within most major bathymetric troughs during full-glacial conditions (Fig. 7).

For the Bear Island trough ice stream, an ice velocity of about 800 m yr^{-1} was calculated for 15 ka (Fig. 7). This ice stream drained ice at a rate of 32 km^3 yr^{-1}, representing by far the largest outlet of ice from the Eurasian Arctic ice sheet (Table 2). Assuming that the Bear Island ice stream had a deformable bed, we calculated the volume of sediment transported to the continental margin through the deformation of basal sediments during the late Weichselian glacial period. A sedimentation rate of 2–4 cm yr^{-1} was predicted along the mouth of the Bear Island trough between 27 and 14 ka (Fig. 9). This is equivalent to 0.07–0.13 cm yr^{-1} averaged over the fan. Similarly, high delivery rates of 2–6 cm yr^{-1} of glacial sediments (equivalent to 0.2–0.6 cm yr^{-1} averaged over the fan) were predicted between 27 and 12 ka at the mouth of the Storfjorden trough (Fig. 9). The modeled volumes of sediment that accumulated at the continental margin of the Bear Island and Storfjorden troughs (4600 km^3 and 900 km^3) (Fig. 10) are similar to the volumes of late Weichselian sediment measured over the respective fans using seismic methods (4200 km^3 and 700 km^3). The model also predicts that major glacier-fed fan systems would have built up on the northern, Arctic Ocean margin of the Barents and Kara Seas, particularly on the continental slope adjacent to the St. Anna and Franz-Victoria troughs (Fig. 9). One major cross-shelf trough draining ice to the Arctic Ocean, the St. Anna trough, is predicted to deliver sediments at a rate that produces a fan intermediate in size between those offshore of the Bear Island and Storfjorden troughs (Figs. 9 and 10A). These glacial sediments are then distributed over the large submarine fans mainly by gravity-driven slope processes, and both side-scan sonar and seismic investigations have shown that a series of stacked debris flow make up the major building blocks of these fan systems (e.g., Vorren et al., 1989, 1998; Hjelstuen et al., 1996; Dowdeswell et al., 1996a; Elverhøi et al., 1997).

ACKNOWLEDGMENTS

Supported by United Kingdom Natural Environment Research Council (NERC) grant GR3/8508 and European Union of Marine Science and Technology (EU MAST) III ENAM II grant MAS3-CT-95-0003 to Dowdeswell and a Nuffield Foundation grant to Siegert. This work is a contribution to the European North Atlantic Margins Programme (ENAM II) and to the European Science Foundation Programme on Quaternary Environments of the Eurasian North (QUEEN). We thank S. Anandakrishnan for reviewing this paper.

REFERENCES CITED

Alley, R. B., 1990, Multiple steady states in ice-water-till systems: Annals of Glaciology, v. 14, p. 1–5.

Alley, R. B., Blankenship, D. D., Rooney, S. T., and Bentley, C. R., 1989, Sedimentation beneath ice shelves: The view from Ice Stream B: Marine Geology, v. 85, p. 101–120.

Andersen, E. S., Dokken, T. M., Elverhøi, A., Solheim, A., and Fossen, I., 1996, Late Quaternary sedimentation and glacial history of the western Svalbard continental margin: Marine Geology, v. 133, p. 123–156.

Arnold, N., and Sharp, M., 1992, Influence of glacier hydrology on the dynamics of a large Quaternary ice sheet: Journal of Quaternary Science, v. 7, p. 109–124.

Barrett, P. J., 1991, Antarctica and global climatic change: A geological perspective, *in* Harris, C. M., and Stonehouse, B., eds., Antarctica and global climate change: London, Belhaven Press, and the Scott Polar Research Institute, p. 35–50.

Bentley, C. R., 1987, Antarctic ice streams: A review: Journal of Geophysical Research, v. 92, p. 8843–8858.

Blanksenship, D. D., Bentley, C. R., Rooney, S. T., and Alley, R. B., 1986, Seismic measurements reveal a saturated porous layer beneath an active Antarctic ice stream: Nature, v. 332, p. 54–57.

Blanksenship, D. D., Bentley, C. R., Rooney, S. T., and Alley, R. B., 1987, Till beneath Ice Stream B. 1. Properties derived from seismic travel times: Journal of Geophysical Research, v. 92, p. 8903–8912.

Boulton, G. S., 1990, Sedimentary and sea level changes during glacial cycles and their control on glacimarine facies architecture, *in* Dowdeswell, J. A., and Scourse, J. D., eds., Glacimarine environments: Processes and sediments: Geological Society [London] Special Publication 53, p. 15–52.

Boulton, G. S., and Jones, A. S., 1979, Stability of temperate ice sheets resting on beds of deformable sediments: Journal of Glaciology, v. 42, p. 29–43.

Boulton, G. S., and Hindmarsh, R. C. A., 1987, Sediment deformation beneath glaciers: Rheology and geological consequences: Journal of Geophysical Research, v. 92, p. 9059–9082.

Bugge, T., Belderson, R. H., and Kenyon, N. H., 1988, The Storegga slide: Royal Society of London Philosophical Transactions, ser. A, v. 325, p. 357–388.

Dowdeswell, J. A., 1986, Drainage-basin characteristics of Nordanstlandet ice caps, Svalbard: Journal of Glaciology v. 32, p. 31–38.

Dowdeswell, J. A., 1995, Glaciers in the High Arctic and recent environmental change: Royal Society of London Philosophical Transactions, ser. A, v. 352, p. 321–334.

Dowdeswell, J. A., and Collin, R. L., 1990, Fast-flowing outlet glaciers on Svalbard ice caps: Geology, v. 18, p. 778–781.

Dowdeswell, J. A., Drewry, D. J., Cooper, A. P. R., Gorman, M. R., Liestøl, O., and Orheim, O., 1986, Digital mapping of the Nordaustlandet ice caps from airborne geophysical investigations: Annals of Glaciology, v. 8, p. 51–58.

Dowdeswell, J. A., Kenyon, N. H., Elverhøi, A., Laberg, J. S., Hollender, F.-J., Mienert, J., and Siegert, M. J., 1996a, Large-scale sedimentation on the glacier-influenced Polar North Atlantic margins: Long-range side-scan sonar evidence: Geophysical Research Letters, v. 23, p. 3535–3538.

Dowdeswell, J. A., Gorman, M. R., Glazovsky, A. F., and Macheret, Y. Y., 1996b, Airborne radio-echo sounding of the ice caps on Franz Josef Land in 1994: Materialy Glyatsiologicheskikh Issledovaniy, Khronika, v. 80, p. 248–254.

Dowdeswell, J. A., Kenyon, N. H., and Laberg, J. S., 1997a, The glacier-influenced Scoresby Sund Fan, East Greenland continental margin: Evidence from GLORIA and 3.5 kHz records: Marine Geology, v. 143, p. 207–221.

Dowdeswell, J. A., Kenyon, N. H., Laberg, J. S., and Elverhøi, A., 1997b, Submarine debris flows on glacier-influenced margins: GLORIA imagery of the Bear Island Fan, *in* Davies, T. A., Bell, T., Cooper, A. K., Jozenhans, H., Polyak, L., Solheim, A., Stoker, M., and Stravers, J. A., eds., Acoustic images of glaciated continental margins: London, Chapman and Hall, p. 118–119.

Dowdeswell, J. A., Unwin, B., Nuttall, A.-M., and Wingham, D. J., 1999, Velocity structure, flow instability and mass flux on a large Arctic ice cap from satellite radar interferometry: Earth and Planetary Science Letters, v. 167, p. 131–140.

Elverhøi, A., and Solheim, A., 1983, The Barents Sea ice sheet: A sedimentological discussion: Polar Research, v. 1, p. 23–42.

Elverhøi, A., Fjeldskaar, W., Solheim, A., Nyland-Berg, M., and Russwurm, L., 1993, The Barents Sea Ice Sheet: A model of its growth and decay during the last ice maximum: Quaternary Science Reviews, v. 12, p. 863–873.

Elverhøi, A., Anderson, E. S., Dokken, T., Hebbeln, D., Spielhagen, R., Svendsen, J. I., Sørflaten, M., Rørnes, A., Hald, M., and Forsberg, C. F., 1995, The growth and decay of the Late Weichselian ice sheet in western Svalbard and adjacent areas based on provenance studies of marine sediments: Quaternary Research, v. 44, p. 303–316.

Elverhøi, A., Norem, H., Andersen, E. S., Dowdeswell, J. A., Fossen, I., Haflidason, H., Kenyon, N. H., Laberg, J. S., King, E. L., Sejrup, H. P., Solheim, A., and Vorren, T., 1997, On the origin and flow behavior of submarine slides on deep-sea fans along the Norwegian-Barents Sea continental margin: Geo-Marine Letters, v. 17, p. 119–125.

Fairbanks, R. G., 1989, A 17 000-year glacio-eustatic sea level record: Influence of glacial melting rates on the Younger Dryas event and deep ocean circulation: Nature, v. 342, p. 637–643.

Faleide, J. I., Solheim, A., Fiedler, A., Hjelstuen, B. O., Andersen, E. S., and Vanneste, K., 1996, Late Cenozoic evolution of the western Barents Sea–Svalbard continental margin: Global and Planetary Change, v. 12, p. 53–74.

Fiedler, A., and Faleide, J. I., 1996, Cenozoic sedimentation along the southwestern Barents Sea margin in relation to uplift and erosion of the shelf: Global and Planetary Change, v. 12, p. 75–93.

Fleming, K. M., Dowdeswell, J. A., and Oerlemans, J., 1997, Modelling the mass balance of north-west Spitsbergen glaciers and responses to climate change: Annals of Glaciology, v. 24, p. 203–210.

Forman, S. L., 1990, Postglacial relative sea-level history of northwestern Spitsbergen, Svalbard: Geological Society of America Bulletin, v. 102, p. 1580–1590.

Forman, S. L., Lubinski, D., Miller, G. H., Snyder, J., Matishov, G., Korsun, S., and Myslivets, V., 1995, Postglacial emergence and distribution of late Weichselian ice-sheet loads in the northern Barents and Kara Seas, Russia: Geology, v. 23, p. 113–116.

Fortuin, J. P. F., and Oerlemans, J., 1990, Parameterization of the annual surface temperature and mass balance of Antarctica: Annals of Glaciology, v. 14, p. 78–84.

Grosswald, M. G., and Hughes, T. J., 1995, Paleoglaciology's grand unsolved problem: Journal of Glaciology, v. 41, p. 313–332.

Hagen, J. O., and Liestøl, O., 1990, Long-term glacier mass-balance investigations in Svalbard, 1950–1988: Annals of Glaciology, v. 14, p. 102–106.

Hebbeln, D., Dokken, T., Andersen, E. S., Hald, M., and Elverhøi, A., 1994, Moisture supply for northern ice-sheet growth during the Last Glacial Maximum: Nature, v. 370, p. 357–360.

Hebbeln, D., Henrich, R., and Baumann, K.-H., 1998, Paleoceanography of the last interglacial/glacial cycle in the Polar North Atlantic: Quaternary Science Reviews, v. 17, p. 125–153.

Hisdal, V., 1985, Geography of Svalbard: Oslo, Norsk Polarinstitutt, Polarhandbok 2, 75 p.

Hjelstuen, B. O., Elverhøi, A., and Faleide, J. I., 1996, Cenozoic erosion and sediment yield in the drainage area of the Storfjorden Fan: Global and Planetary Change, v. 12, p. 95–117.

Hooke, R. L., and Elverhøi, A., 1996, Sediment flux from a fjord during glacial periods, Isfjorden, Spitsbergen: Global and Planetary Change, v. 12, p. 237–249.

Hughes, T. J., 1992, Theoretical calving rates from glaciers along ice walls grounded in water of variable depths: Journal of Glaciology, v. 38, p. 282–294.

Jansen, E., and Sjøholm, J., 1991, Reconstruction of glaciation over the past 6 Myr from ice-borne deposits in the Norwegian Sea: Nature, v. 349, p. 600–603.

King, E. L., Sejrup, H. P., Haflidason, H., Elverhøi, A., and Aarseth, I., 1996, Quaternary seismic stratigraphy of the North Sea Fan: Glacially-fed gravity flow aprons, hemipelagic sediments, and large submarine slides: Marine Geology, v. 130, p. 293–316.

Koç, N., Jansen, E., and Haflidason, H., 1993, Paleoceanographic reconstructions of surface ocean conditions in the Greenland, Iceland and Norwegian Seas through the last 14 ka based on diatoms: Quaternary Science Reviews, v. 12, p. 115–140.

Laberg, J. S., and Vorren, T. O., 1995, Late Weichselian debris flow deposits on the Bear Island trough mouth fan: Marine Geology, v. 127, p. 45–72.

Laberg, J. S., and Vorren, T. O., 1996a, The middle and late Pleistocene evolution of the Bear Island trough mouth fan: Global and Planetary Change, v. 12, p. 309–330.

Laberg, J. S., and Vorren, T. O., 1996b, The glacier-fed fan at the mouth of Storfjorden Trough, western Barents Sea: A comparative study: Geologische Rundschau, v. 85, p. 338–349.

Lambeck, K., 1995, Constraints on the Late Weichselian Ice Sheet over the Barents Sea from observations of raised shorelines: Quaternary Science Reviews, v. 14, p. 1–16.

Lambeck, K., 1996, Limits on the areal extent of the Barents Sea Ice Sheet in Late Weichselian time: Global and Planetary Change, v. 12, p. 41–51.

MacAyeal, D. R., 1992, Irregular oscillations of the West Antarctic ice sheet: Nature, v. 359, p. 29–32.

Mahaffy, M. W., 1976, A three-dimensional numerical model of ice sheets: Tests on the Barnes Ice Cap, Northwest Territories: Journal of Geophysical Research, v. 81, p. 1059–1066.

Manabe, S., and Bryan, K., Jr., 1985, CO_2-induced change in a coupled ocean-atmosphere model, and its paleoclimatic implications: Journal of Geophysical Research, v. 90, p. 11689–11707.

Mangerud, J., and Svendsen, J. I., 1992, The last interglacial/glacial period on Spitsbergen, Svalbard: Quaternary Science Reviews, v. 11, p. 633–664.

Mienert, J., Kenyon, N. H., Thiede, J., and Hollender, F.-J., 1993, Polar continental margins: Studies off East Greenland: Eos (Transactions, American Geophysical Union), v. 74, p. 225, 234, 236.

Murray, T., 1990, Deformable glacier beds: Measurement and modelling [Ph.D. dissert.]: Aberystwyth, University College of Wales, 321 p.

Oerlemans, J., and van der Veen, C. J., 1984, Ice sheets and climate: Dordrecht, Reidel, 216 p.

Paterson, W. S. B., 1994, The Physics of glaciers. London, Pergamon Press, 480 p.

Payne, A. J., Sugden, D. E., and Clapperton, C. M., 1989, Modeling the growth and decay of the Antarctic Peninsula Ice Sheet: Quaternary Research, v. 31, p. 119–134.

Pelto, M. S., and Warren, C. R., 1991, Relationship between tidewater glacier calving velocity and water depth at the calving front: Annals of Glaciology, v. 15, p. 115–118.

Pelto, M. S., Higgins, S. M., Hughes, T. J., and Fastook, J. L., 1990, Modeling mass-balance changes during a glaciation cycle: Annals of Glaciology, v. 14, p. 238–241.

Polyak, L., Forman, S. L., Herlihy, F. A., Ivanov, G., and Krinitsky, P., 1997, Late Weichselian deglacial history of the Svyataya (Saint) Anna Trough, northern Kara Sea, Arctic Russia: Marine Geology, v. 143, p. 169–188.

Rose, K. E., 1979, Characteristics of ice flow in Marie Byrd Land, Antarctica: Journal of Glaciology, v. 24, p. 63–75.

Sættem, J., Poole, D. A. R., Ellingsen, K. L., and Sejrup, H. P., 1992, Glacial geology of outer Bjørnøyrenna, southwestern Barents Sea: Marine Geology, v. 103, p. 15–51.

Salvigsen, O., Forman, S. L., and Miller, G. H., 1992, Thermophilous molluscs on Svalbard during the Holocene and their paleoclimatic implications: Polar Research, v. 11, p. 1–10.

Siegert, M. J., 1993, Numerical modelling studies of the Svalbard-Barents Sea Ice Sheet [Ph.D. dissert.]: Cambridge, University of Cambridge, 287 p.

Siegert, M. J., and Dowdeswell, J. A., 1995, Numerical modeling of the Late Weichselian Svalbard–Barents Sea Ice Sheet: Quaternary Research, v. 43, p. 1–13.

Siegert, M. J., and Dowdeswell, J. A., 1996, Topographic control on the dynamics of the Svalbard–Barents Sea Ice Sheet: Global and Planetary Change, v. 12, p. 27–39.

Simões, J. C., 1990, Environmental interpretation from Svalbard ice cores [Ph.D. dissert.]: Cambridge, University of Cambridge, 236 p.

Solheim, A., Riis, F., Elverhøi, A., Faleide, J. I., Jensen, L. N., and Cloetingh, S., 1996, Impact of glaciations on basin evolution: Data and models from the Norwegian margin and adjacent areas—Introduction and summary: Global and Planetary Change, v. 12, p. 1–10.

Vågnes, E., 1996, Cenozoic deposition in the Nansen Basin, a first-order estimate based on present-day bathymetry: Global and Planetary Change, v. 12, p. 149–157.

Vogt, P. R., Crane, K., and Sundvor, E., 1993, Glacigenic mudflows on the Bear Island submarine fan: Eos (Transactions, American Geophysical Union), v. 74, p. 449, 452, 453.

Vorren, T. O., Vorren, K.-D., Alm, T., Gulliksen, S., and Løvlie, R., 1988, The last deglaciation (20 000 to 11 000 BP) on Andøya, northern Norway: Boreas, v. 17, p. 41–77.

Vorren, T. O., Lebesbye, E., Andreassen, K., and Larsen, K.-B., 1989, Glacigenic sediments on a passive continental margin as exemplified by the Barents Sea: Marine Geology, v. 85, p. 251–272.

Vorren, T. O., Lebesbye, E., and Larsen, K. B., 1990, Geometry and genesis of the glacigenic sediments in the southern Barents Sea, *in* Dowdeswell, J. A., and Scourse, J. D., eds., Glacimarine environments: Processes and sediments: Geological Society [London] Special Publication 53, p. 253–268.

Vorren, T. O., Laberg, J. S., Blaume, F., Dowdeswell, J. A., Kenyon, N. H., Mienert, J., Rumohr, J., and Werner, F., 1998, The Norwegian-Greenland Sea continental margins: Morphology and late Quaternary sedimentary processes and environment: Quaternary Science Reviews, v. 17, p. 273–302.

MANUSCRIPT RECEIVED BY THE SOCIETY OCTOBER 15, 1997
REVISED MANUSCRIPT RECEIVED SEPTEMBER 21, 1998
MANUSCRIPT ACCEPTED OCTOBER 10, 1998

Printed in U.S.A.